Plant Communications
Research article

CellPress
Partner Journal

Dissection of a rapidly evolving wheat resistance gene cluster by long-read genome sequencing accelerated the cloning of *Pm69*

Yinghui Li[1,2,11], Zhen-Zhen Wei[1,2,3,11], Hanan Sela[1,2], Liubov Govta[1,2], Valentyna Klymiuk[1,2,4], Rajib Roychowdhury[1,2], Harmeet Singh Chawla[4,9], Jennifer Ens[4], Krystalee Wiebe[4], Valeria Bocharova[1,2], Roi Ben-David[1,2,5], Prerna B. Pawar[1,2], Yuqi Zhang[6], Samidha Jaiwar[1,2], István Molnár[7,10], Jaroslav Doležel[7], Gitta Coaker[8], Curtis J. Pozniak[4] and Tzion Fahima[1,2,*]

[1]Institute of Evolution, University of Haifa, Mt. Carmel, Haifa 3498838, Israel

[2]The Department of Evolutionary and Environmental Biology, University of Haifa, Mt. Carmel, Haifa 3498838, Israel

[3]The Institute of Plant Protection, Sichuan Academy of Agricultural Sciences, Chengdu 610066, China

[4]Crop Development Centre and Department of Plant Sciences, University of Saskatchewan, 51 Campus Drive, Saskatoon, SK S7N 5A8, Canada

[5]Department of Vegetables and Field Crops, Institute of Plant Sciences, Agricultural Research Organization (ARO) – Volcani Center, Rishon Lezion 7505101, Israel

[6]Department of Crop Genomics and Bioinformatics, China Agricultural University, Beijing 100094, China

[7]Institute of Experimental Botany of the Czech Academy of Sciences, Centre of the Region Haná for Biotechnological and Agricultural Research, Šlechtitelů 31, 779 00 Olomouc, Czech Republic

[8]Plant Pathology Department, University of California, Davis, Davis, CA 95616, USA

[9]Present address: Department of Plant Science, University of Manitoba, Winnipeg, MB R3T 2N2, Canada

[10]Present address: Agricultural Institute, Centre for Agricultural Research, ELKH, Martonvásár 2462, Hungary

[11]These authors contributed equally to this article.

***Correspondence: Tzion Fahima (tfahima@evo.haifa.ac.il)**

https://doi.org/10.1016/j.xplc.2023.100646

ABSTRACT

Gene cloning in repeat-rich polyploid genomes remains challenging. Here, we describe a strategy for overcoming major bottlenecks in cloning of the powdery mildew resistance gene (R-gene) *Pm69* derived from tetraploid wild emmer wheat. A conventional positional cloning approach was not effective owing to suppressed recombination. Chromosome sorting was compromised by insufficient purity. A *Pm69* physical map, constructed by assembling Oxford Nanopore Technology (ONT) long-read genome sequences, revealed a rapidly evolving nucleotide-binding leucine-rich repeat (NLR) R-gene cluster with structural variations. A single candidate NLR was identified by anchoring RNA sequencing reads from susceptible mutants to ONT contigs and was validated by virus-induced gene silencing. *Pm69* is likely a newly evolved NLR and was discovered in only one location across the wild emmer wheat distribution range in Israel. *Pm69* was successfully introgressed into cultivated wheat, and a diagnostic molecular marker was used to accelerate its deployment and pyramiding with other R-genes.

Li Y., Wei Z.-Z., Sela H., Govta L., Klymiuk V., Roychowdhury R., Chawla H.S., Ens J., Wiebe K., Bocharova V., Ben-David R., Pawar P.B., Zhang Y., Jaiwar S., Molnár I., Doležel J., Coaker G., Pozniak C.J., and Fahima T. (2024). Dissection of a rapidly evolving wheat resistance gene cluster by long-read genome sequencing accelerated the cloning of *Pm69*. Plant Comm. **5**, 100646.

INTRODUCTION

Powdery mildew (PM) caused by the biotrophic fungus *Blumeria graminis* f. sp. *tritici* (*Bgt*) is one of the most destructive wheat diseases worldwide. To date, more than 60 official *Pm* resistance genes (*Pm1–Pm68*) have been identified and mapped in wheat and its wild relatives, of which only 12 have been cloned (McIntosh et al., 2020). *Pm3b*/*Pm8*/*Pm17*, *Pm2a*, *Pm21*/*Pm12*, *Pm60*/*MlIW172*/*MlWE18*, *Pm5e*, *Pm41*, and *Pm1a* encode nucleotide-binding leucine-rich repeat (NLR) proteins (Yahiaoui et al., 2004; Hurni et al., 2013; Sánchez-Martín et al., 2016;

Published by the Plant Communications Shanghai Editorial Office in association with Cell Press, an imprint of Elsevier Inc., on behalf of CSPB and CEMPS, CAS.

This is an open access article under the CC BY-NC-ND license (http://creativecommons.org/licenses/by-nc-nd/4.0/).

Singh et al., 2018; Xing et al., 2018; Zou et al., 2018; Li et al., 2020; Xie et al., 2020; Hewitt et al., 2021a; Wu et al., 2021, 2022; Zhu et al., 2023). *Pm24* and *WTK4* encode tandem kinase proteins (Lu et al., 2020; Gaurav et al., 2022). *Pm4* encodes a putative chimeric protein of a serine/threonine kinase, multiple C2 domains, and transmembrane regions (Sánchez-Martín et al., 2021). *Pm38* (*Lr34/Yr18/Sr57*, ABC transporter) and *Pm46* (*Lr67/Yr46/Sr55*, hexose transporter) show broad-spectrum adult-plant resistance to PM and rust diseases (Krattinger et al., 2009; Moore et al., 2015). However, *Pm* resistance genes are frequently overcome because of the rapid evolution of *Bgt* isolates (Golzar et al., 2016). Thus, identification and cloning of novel disease resistance genes (R-genes) and their deployment into cultivated wheat germplasm can enrich the repertoire of genes available for resistance breeding.

Positional cloning has been widely used to clone plant genes. Published reference genomes serve as powerful tools for dissection of target genomic regions and provide a reliable resource for candidate gene prediction (Walkowiak et al., 2020). However, genes responsible for the phenotype of interest may be absent from reference genotypes, especially when the target genes are derived from wild relatives (Bohra et al., 2021). Robust R-genes, encoding intracellular immune receptors with NLR domain architecture, are frequently arranged in gene clusters that are likely formed by tandem duplications (Andersen et al., 2020). Such clusters of highly similar genes make it particularly challenging to localize a causal NLR. Construction of a bacterial artificial chromosome (BAC) library with a 100–200 kb insert size may be useful for assembling high-quality physical maps to support positional cloning (Shizuya et al., 1992); however, this technology is time and labor intensive, especially when working with complex genomes such as wheat.

Several methods for cloning novel R-genes in complex polyploid genomes have been developed based on next-generation sequencing (NGS) (Zhang et al., 2020). These methods include mutagenesis and R-gene enrichment and sequencing (MutRenSeq) (Steuernagel et al., 2016), association genetics with R-gene enrichment sequencing (AgRenSeq) (Arora et al., 2019), mutant chromosome flow sorting and short-read sequencing (MutChromSeq) (Sánchez-Martín et al., 2016), and targeted chromosome-based cloning via long-range assembly (TACCA) (Thind et al., 2017). Nonetheless, these methods still have some limitations. For example, MutRenSeq and AgRenSeq identify only NLR genes, and MutChromSeq and TACCA rely on the purification of individual chromosomes (Molnár et al., 2014; Zhang et al., 2020). However, k-mer-based association mapping can overcome this limitation and has recently been used to clone the non-NLR *Pm* R-gene *WTK4* (Gaurav et al., 2022). Bulked segregant RNA sequencing (BSR-Seq) and bulked segregant core genome targeted sequencing (CGT-Seq) have also been used to identify R-genes, although these methods may yield many candidates (Xie et al., 2020; Wu et al., 2021).

Wheat has a large and complex genome with more than 85% repetitive sequences, making its sequence assembly challenging (International Wheat Genome Sequencing Consortium et al., 2018), particularly when using short-read (100–250 bp) sequencing technologies. Recently developed long-read sequencing platforms such as Pacific Biosciences (PacBio) single-molecule real-time sequencing and Oxford Nanopore Technology (ONT) sequencing generate long (>10 kb) reads that result in more contiguous sequence assemblies (Rhoads and Au, 2015; Deamer et al., 2016). Long-read sequencing technologies have been successfully used for genome assemblies of barley, *Aegilops tauschii*, and bread wheat (Mascher et al., 2021; Sato et al., 2021; Zhou et al., 2021; Athiyannan et al., 2022; Aury et al., 2022; Li et al., 2022). These technologies can significantly improve physical mapping, detection of structural variants, and transcript isoform identification (Amarasinghe et al., 2020; Nilsen et al., 2020; Walkowiak et al., 2020).

Wild emmer wheat (WEW; *Triticum turgidum* ssp. *dicoccoides*, $2n = 4x = 28$, AABB), the tetraploid progenitor of hexaploid bread wheat (*T. aestivum*, $2n = 6x = 42$, AABBDD), is a valuable genetic resource for R-genes. More than 20 *Pm* R-genes have been identified and mapped in WEW (Klymiuk et al., 2019), but only *Pm41* on chromosome arm 3BL and *TdPm60* on chromosome arm 7AL have been cloned. *Pm41* and *TdPm60* frequencies in tested WEW collections were 1.81% and 25.6%, respectively (Li et al., 2020, 2021; Wu et al., 2022). *Pm69* (*PmG3M*), a dominant gene that confers wide-spectrum resistance to *Bgt* isolates, is the only gene mapped to the telomeric region of chromosome arm 6BL in WEW (Xie et al., 2012; Wei et al., 2020).

In the current study, we describe the winding road to cloning a gene in the complex wheat genome, overcoming the challenges of rearrangements and NLR clusters. We developed an advanced approach that combines whole genome long-read sequencing and RNA sequencing (RNA-seq) of susceptible ethyl methane sulfonate (EMS) mutants. A single candidate NLR was identified and validated using virus-induced gene silencing (VIGS). *Pm69* resides in a rapidly evolving NLR cluster, and it is an ‘‘orphan gene’’ found in only one location across the distribution range of natural WEW populations. *Pm69* has been introgressed into a cultivated wheat background and pyramided with the yellow rust R-gene *Yr15*.

RESULTS

Challenges of chromosome walking in a complex, structurally variable region

A recombinant inbred line (RIL) mapping population segregating for *Pm69* was generated by crossing the susceptible durum wheat (*Triticum turgidum* ssp. *durum*) Langdon (LDN) with the resistant WEW accession G305-3M. G305-3M and the F_1 generation (G305-3M × LDN) showed post-haustorial immune responses to *Bgt* #70, accompanied by intracellular reactive oxygen species (ROS) production and host cell death, whereas LDN showed a highly susceptible response, resulting in the development of pronounced fungal pathogen colonies (Figure 1A). G305-3M showed wide-spectrum resistance against 55 tested *Bgt* isolates originating from Asia, Europe, North America, and South America (Supplemental Table 1). For fine mapping of *Pm69*, we screened 5500 F_2 (11 000 gametes) plants with the DNA markers *uhwk386* and *uhwk399* to develop 147 F_{4-7} RILs that carried informative recombination events within the target gene region. In total, 33 additional DNA markers were developed and mapped within this genetic region

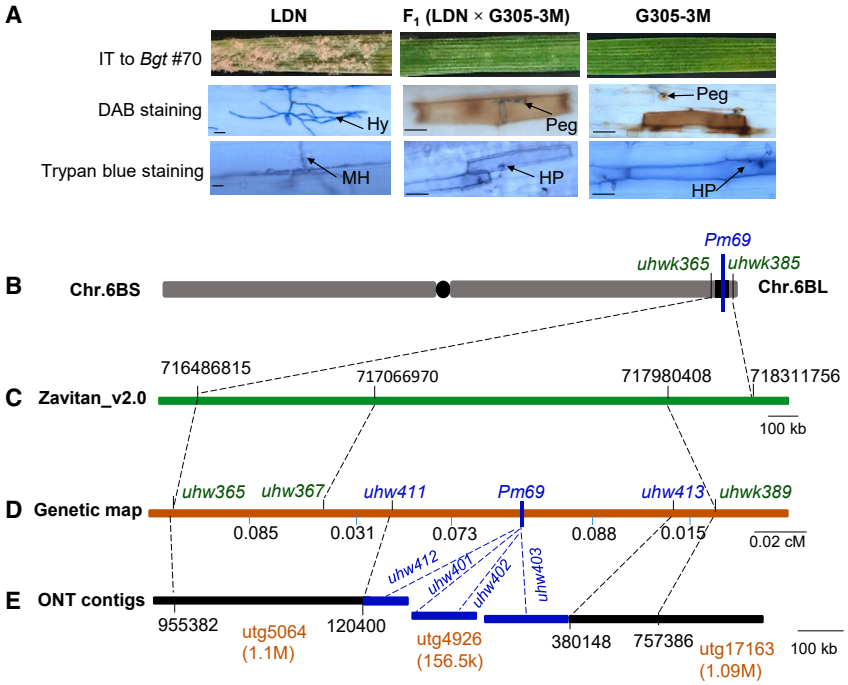

Figure 1. Fine mapping of *Pm69* derived from WEW G305-3M.

(A) Infection types (ITs) of the WEW accession G305-3M (0, highly resistant), the *T. durum* line LDN (4, highly susceptible), and their F_1 progeny (0, highly resistant) to *Bgt* #70 at 7 days post-infection (dpi); DAB staining of leaves at 3 dpi was performed to detect ROS accumulation, visualized as reddish-brown coloration; trypan blue staining of leaves at 3 dpi was performed to detect fungal structures and plant cell death, visualized as blue coloration. MH, mature haustorium; HP, haustorial primordium; Hy, hyphae. Scale bars: 50 μm.

(B) The *Pm69* gene region on the long arm of wheat chromosome 6B.

(C) Locations of *Pm69*-flanking genetic markers on the Zavitan WEW_v.2.0 reference genome.

(D) Genetic map of *Pm69*. The green markers were developed using WEW_v.2.0 sequences, and the blue markers were developed using ONT contigs.

(E) G305-3M ONT assembly contigs mapped to the *Pm69* gene region. The physical interval of the *Pm69* gene region on ONT contigs is marked in blue.

(Supplemental Figure 1), enabling us to map *Pm69* within a 0.21-centimorgan (cM) interval between markers *uhw367* and *uhwk389* (Figure 1; Supplemental Tables 2 and 3).

Anchorage of markers closely linked to *Pm69* to three wheat reference genomes revealed higher collinearity with the Zavitan WEW_v.2.0 assembly than with those of durum wheat Svevo (RefSeq Rel. 1.0) and bread wheat Chinese Spring (International Wheat Genome Sequencing Consortium [IWGSC] RefSeq v.1.0) (Supplemental Figure 2). As Zavitan, Svevo, and Chinese Spring are susceptible to *Bgt* #70 (Supplemental Figure 3), we did not expect to find their functional *Pm69* candidates. In Zavitan, this region spans 1.02 Mb and contains 23 genes, 18 of which are NLRs (Supplemental Table 4). However, 10 markers physically mapped to this region showed co-segregation with the *Pm69* phenotype, suggesting that recombination is suppressed (Supplemental Figure 1). In addition, 12 markers developed based on these candidate genes amplified PCR products in the susceptible parent LDN but not in the *Pm69* donor line G305-3M (Supplemental Table 5). Taken together, these results indicated that structural variation between G305-3M and LDN probably caused suppression of recombination around the *Pm69* gene region and thus prevented further chromosome walking toward *Pm69* based on published reference genomes.

Challenges of using MutChromSeq based on chromosome sorting in tetraploid wheat

As an alternative approach, we attempted to use MutChromSeq to clone *Pm69* (Sánchez-Martín et al., 2016). To produce *pm69* loss-of-function mutants, we used EMS treatment to mutagenize the resistant WEW accession G305-3M and F_{7-8} RILs. A total of five independent susceptible mutant lines (four in the G305-3M background and one in a resistant RIL background) were identified and grown to the M_4 generation (Supplemental Figure 4).

We then attempted to isolate 6B chromosomes from G305-3M and LDN by flow cytometry–based chromosome sorting. Because of their similar size and similar GAA microsatellite content, chromosomes 6B, 1B, 7B, 4B, and 5B formed a composite, poorly resolved population upon bivariate flow karyotyping (Supplemental Figure 5). We sorted chromosomes from the composites in hopes of further enriching chromosome 6B but were able to achieve maximum purities of only 47% and 51% in G305-3M and LDN, respectively, with contamination from other chromosomes (Supplemental Figure 5).

We made an additional attempt to flow sort chromosome 6B from the hexaploid introgression line SC28RRR-26 (a bread wheat introgression line cv. Ruta + *Pm69*) that resulted in a higher purity (73.1%) of chromosome 6B sorting (Supplemental Figure 6). However, at that time, EMS-derived mutants of the introgression line were not yet available, and it would have taken at least a couple of years to create these mutants. Thus, alternative approaches were considered.

Dissection of structural variation complexity by ONT sequencing of G305-3M

ONT long-read sequencing technology offered an attractive alternative with which to rapidly generate long contigs that spanned the *Pm69* genomic interval, thus overcoming difficulties caused by structural variations. ONT sequencing was therefore used for whole-genome sequencing (~23× coverage) of WEW accession G305-3M. After assembling the reads, we obtained 2489 contigs, with an N_{50} value of 11.21 Mb and an N_{90} value of 2.6 Mb (Supplemental Figure 7). The longest contig was 70.65 Mb, and the total length of the genome assembly was 10.02 Gb (Supplemental Table 6), which is typical for the tetraploid wheat genome (Avni et al., 2017; Maccaferri et al., 2019).

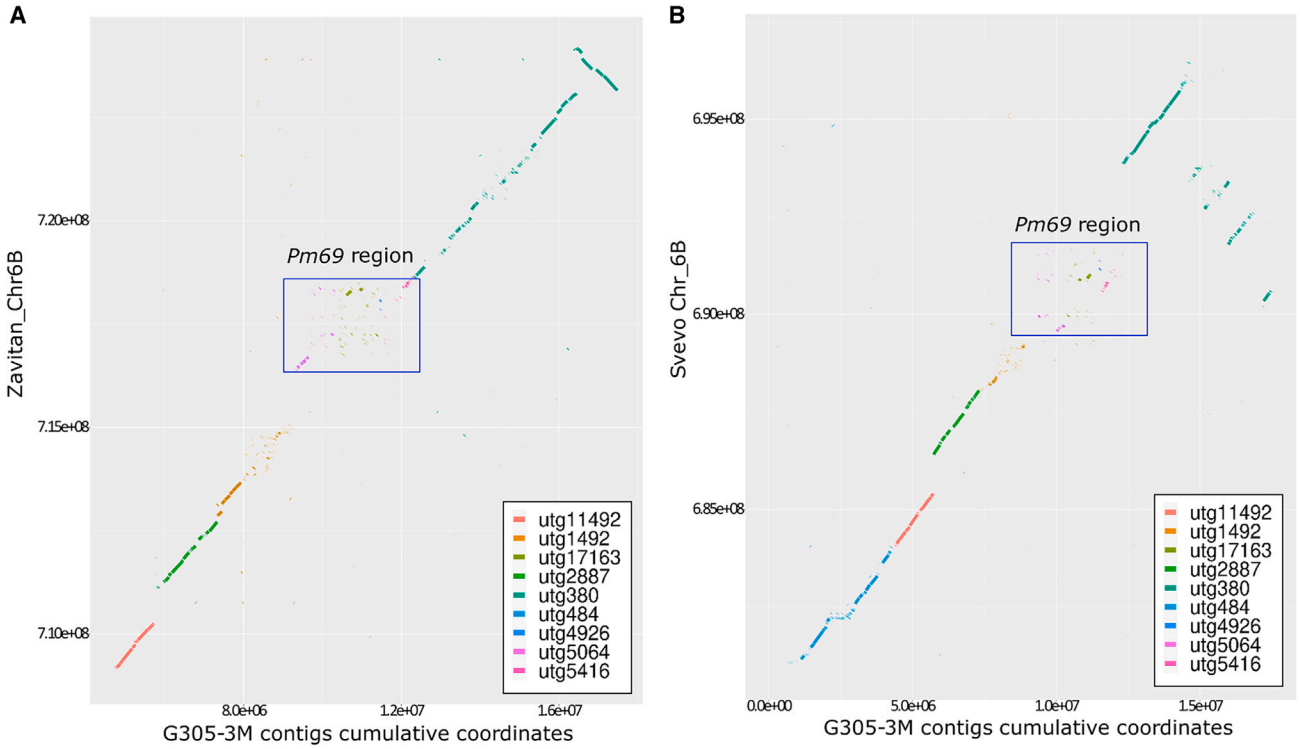

Figure 2. Comparisons of the G305-3M ONT contigs with the 6B pseudomolecule of tetraploid wheat genomes around the *Pm69* gene region.

(A) Wild emmer wheat Zavitan reference genome WEW_v.2.0.

(B) Durum wheat Svevo RefSeq Rel. 1.0.

The x axis: cumulative length of G305-3M contigs; the y axis: physical location of 6B pseudomolecule in the reference genomes. Contigs utg380–utg17163 marked with different colors belong to the ONT assembly of G305-3M.

Construction of the *Pm69* physical map using ONT contigs

To construct the *Pm69* physical map, we anchored the ONT contigs to the *Pm69* genetic map using co-dominant PCR markers. Two contigs, utg17163 (1.1 Mb) and utg5064 (1.09 Mb), were perfectly anchored to the genetic map by four *Pm69*-flanking markers. An additional ONT contig, utg4926 (156.5 kb), was identified by searching for gene sequences in the *Pm69* collinear region of the Zavitan WEW_v.2.0 genome (Supplemental Table 7). On the basis of the three identified ONT contigs, we developed 15 markers that were incorporated into the genetic map by graphical genotyping of the RIL population. Finally, the *Pm69* co-segregating genetic markers spanned part of contig utg5064 (120 400 bp to end), all of contig utg4926 (0–156 528 bp), and part of contig utg17163 (0–380 148 bp) (Figure 1; Supplemental Table 8).

A comparison of the G305-3M ONT contigs with the 6B pseudomolecules of the WEW Zavitan and durum Svevo reference genomes showed a very low level of collinearity around the *Pm69* gene region, indicating massive structural rearrangements between them (Figures 2A and 2B, respectively). By contrast, more distant regions flanking *Pm69* showed high collinearity between the G305-3M contigs and the reference genomes (Figures 2A and 2B).

Identification of a *Pm69* candidate gene by ONT-MutRNA-seq

To identify a candidate for *Pm69* in the final physical interval, we mapped RNA-seq reads from the wild type and four independent EMS-derived susceptible mutants onto the G305-3M ONT contigs (Supplemental Table 9). Using this approach that defined as ONT-MutRNA-seq, we identified eight expressed candidate genes in the *Pm69* physical region (flanked by markers *uhw411–uhw413*), seven in utg17163, and one in utg5064, whereas no expressed genes were found in utg4926. Seven candidates were predicted to be NLRs and one to be a FAR1-related sequence transcription factor (Figure 3B; Supplemental Table 10). Only one gene spanning 12 280 bp on G305-3M contig utg17163, named *NLR-6*, had five different point mutations in the four susceptible mutants (Supplemental Figure 8; Supplemental Table 11). These five mutations in *NLR-6* were all G/C-to-A/T transitions typical of EMS mutagenesis, and the remaining seven genes in this region did not have any mutations. In the gene region of G305-M, the expression level of NLR-6 (163 reads/Kbp) extracted from the RNA-seq data was higher than that of the other NLRs, which ranged from 15 to 53 reads/Kbp.

The predicted 2763-bp coding sequence structure of *NLR-6* was validated by Sanger sequencing using G305-3M cDNA.

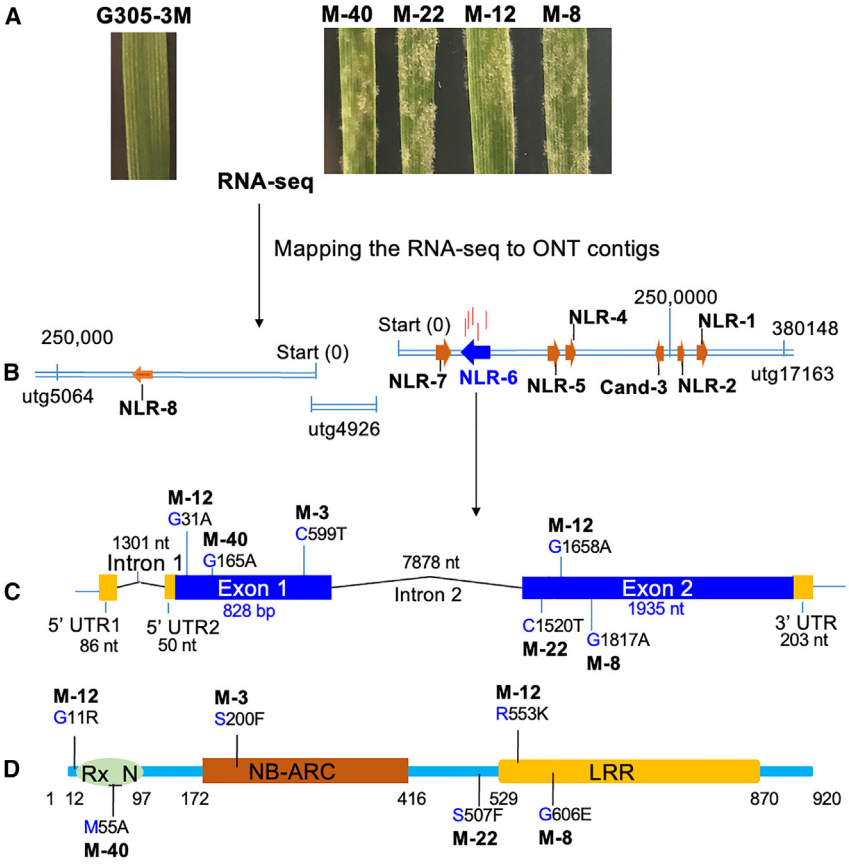

Figure 3. Workflow for identification of *Pm69* on the ONT contigs by MutRNA-seq.

(A) Phenotypes of EMS-derived mutants (M-40, M-22, M-12, and M-18) and the wild type (G305-3M) infected with *Bgt* #70. M-40, M-22, M-12, M-18, and G305-3M were analyzed by RNA-seq to identify SNVs among the three ONT contigs.

(B) Expressed genes in the *Pm69* gene region were identified by aligning the RNA-seq reads to G305-3M ONT contigs. Vertical red lines: the locations of SNVs in the susceptible mutants identified after mapping RNA-seq reads to G305-3M ONT contigs.

(C) Distribution of independent mutations. M-3 was identified by Sanger sequencing.

(D) Predicted structure of the PM69 protein with the coiled-coiled Rx N-terminal domain (Rx_N), nucleotide-binding adaptor shared by Apaf-1, R proteins, and Ced-4 (NB-ARC) domain, leucine-rich repeat (LRR) domain, and precise location of each identified mutation.

The ~12.3-kb genomic region of the gene contains two introns, one located in the 5′ UTR region (Figure 3C). All the identified point mutations in *NLR-6* were validated by Sanger sequencing and were confirmed as missense mutations. Moreover, the resistant sister lines derived from the same M_0 plants harbored the *Pm69* wild-type allele. An additional susceptible mutant line (M-3) identified by Sanger sequencing also contained a point mutation (C599T, protein S200F) in NLR-6 (Figure 3C; Supplemental Table 11). The predicted structure of the NLR-6 protein contains an N-terminal coiled-coil domain, an NB-ARC domain, and an LRR domain (Figure 3D). The coiled-coil domain shows similarity to the N-terminal domain of the potato virus X resistance protein Rx, which has been shown to interact with Ran GTPase-activating protein (RanGAP2), a necessary co-factor in the resistance response (Rairdan et al., 2008). The 3D model of the PM69 protein predicted by AlphaFold v.2.0 (Jumper et al., 2021) showed that all mutations were located within the three important domains or the central alpha helix, likely changing the protein structure and resulting in susceptibility (Supplemental Figure 9).

The expression pattern of *Pm69* (*NLR-6*) was further examined at different time points from 0 to 72 h post-inoculation (hpi) in both non-inoculated (mock) and inoculated G305-3M plants. The expression level of *Pm69* did not change significantly in the *Bgt* #70-infected plants compared with the non-inoculated control from 0 to 16 hpi. However, *Pm69* expression was significantly lower ($p < 0.05$) in the inoculated plants at 16–72 hpi (Supplemental Figure 10).

Functional validation of *Pm69* by VIGS

Barley stripe mosaic virus (BSMV)-induced gene silencing constructs were designed to target two genomic positions in *Pm69* (Supplemental Figure 11). We used a phytoene desaturase (*PDS*) gene-silencing construct to test the efficacy of the VIGS system in tetraploid (G305-3M) and hexaploid (bread wheat introgression line cv. Ruta + *Pm69*) backgrounds. Inoculation with the *Pm69*-silencing constructs resulted in susceptibility to *Bgt* #70 on the 4th–5th leaves in G305-3M and the *Pm69* introgression line, whereas the negative controls showed no visible *Bgt* symptoms on the leaves (Figures 4A and 4B). Silencing of *PDS* produces white streaks resulting from photobleached chlorophyll (Holzberg et al., 2002) (Figure 4A). Histopathological characterization showed that *Pm69* control cells (BSMV:GFP) accumulated intracellular ROS and prevented the invasion of germinating *Bgt* spores. In the *Pm69* VIGS-silenced leaves, because of mosaic silencing, we observed that some germinating *Bgt* spores invaded host cells successfully and developed into *Bgt* colonies, whereas other nearby *Bgt* spores stopped growing owing to ROS activation and cell death responses, suggesting that the resistant and susceptible mosaic reactions occurred side by side. Quantitative reverse transcription PCR (qRT–PCR) showed a significant reduction in expression levels of *Pm69* mRNA in the 4th leaf segments of *Pm69* VIGS-silenced plants compared with *GFP*-silenced plants at 1 week post-virus infection ($p < 0.05$; Figure 4). These results provided functional validation for the role of *Pm69* (NLR-6) in conferring resistance against wheat PM.

Pm69 is a rare allele

A search of 37 published *Triticeae* genome sequences identified 51 PM69 homologs/orthologs from 19 hexaploid wheat, three tetraploid wheat, and six *Aegilops* accessions that showed 82%–89% protein sequence similarity with PM69 (Supplemental Table 12). Most of the PM69 homologs/orthologs were from the 6B and 6D chromosomes. Protein sequence analysis of PM69 homologs/orthologs showed that

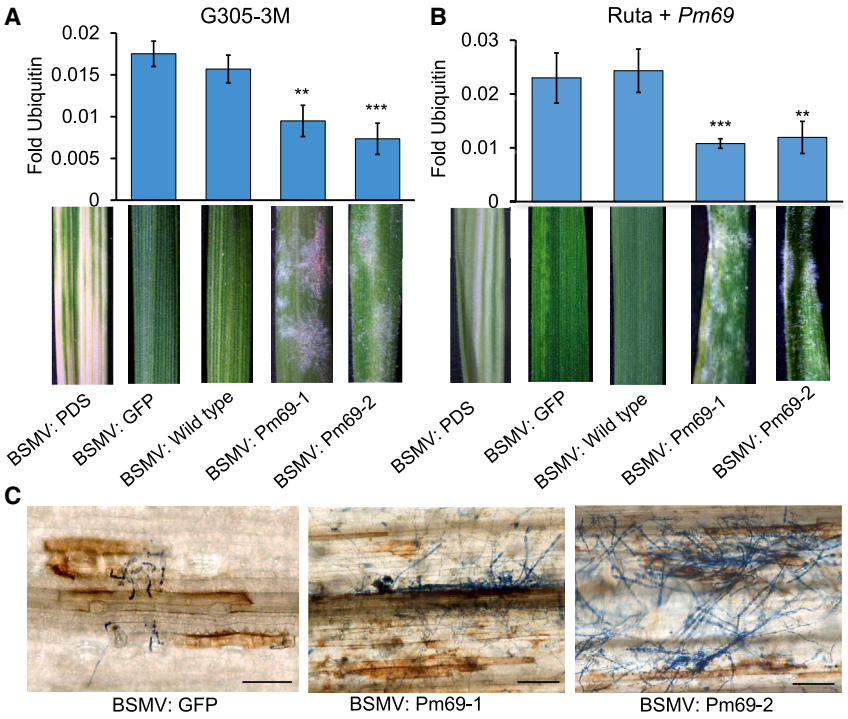

Figure 4. Functional validation of the *Pm69* candidate gene by virus-induced gene silencing (VIGS).

(A) VIGS of the *Pm69* candidate gene in G305-3M.

(B) VIGS of the *Pm69* candidate gene in the introgression line (Ruta+*Pm69*). BSMV:GFP was used as a negative control. BSMV:wild type, the wild type of the *pCa-BSMV-γ* vector, was used as a negative control. BSMV:PDS is the PDS gene-silencing construct used to check the efficiency of the VIGS system; BMSV:Pm69-1 and Pm69-2 are the constructs that targeted the Rx N-terminal domain and the NB-ARC domain, respectively. Asterisks indicate significant differences in *Pm69* expression levels in the 4th leaf segments of target plants compared with the negative control (BSMV:wild type) one week post-virus infection, $^{**}p < 0.01$, $^{***}p < 0.001$ (Student's *t-test*).

(C) Histopathology characterization of *Pm69* wild-type plants (BSMV:GFP) and *Pm69*-silenced plants (BSMV:Pm69-1 and BSMV:Pm69-2). DAB and Coomassie brilliant blue staining of *Pm69*- and *GFP*-silenced leaves of G305-3M at 7 dpi with *Bgt* #70. Scale bars: 100 μm.

they varied mainly in the LRR domain (Supplemental Figures 13 and 14). Phylogenetic and phenotypic analyses showed that the pm69 homologs/orthologs were genetically diverse, and all of them were likely to be non-functional in *Bgt* #70 resistance (Supplemental Figure 13; Supplemental Table 12).

The functional molecular marker *uhw403* was used for large-scale screening of *Pm69* distribution in 536 wheat accessions, of which 310 were WEW and 226 represented other wheat species (Figure 5A; Supplemental Table 13). Only G305-3M produced positive PCR amplification. To further estimate the presence of *Pm69* in the WEW gene pool, we collected 64 additional WEW accessions in a radius of less than 1 km from the original G305-3M collection site (Figure 5B and Supplemental Figure 15). Even there, we were able to find only three WEW accessions that amplified the *uhw403* marker and exhibited strong resistance to *Bgt* #70 (Figures 5B–5D; Supplemental Table 14). Sanger sequencing confirmed that these accessions contained a functional *Pm69* allele identical to that of G305-3M. Moreover, eight resistant accessions were positive for the marker *M-Pm60-S1* (Zhao et al., 2020; Li et al., 2021), suggesting that they carry *TdPm60*. Five other resistant accessions were negative for both *M-Pm60-S1* and *uhw403* markers, suggesting they contain other *Pm* genes. Therefore, we conclude that *Pm69* is a rare NLR allele among WEW collections, even within its population of origin near the collection site of the donor accession G305-3M.

Pm69 is located within a rapidly evolving NLR cluster

Microcollinearity analysis of different wheat genomes revealed high copy-number variation of NLR clusters in the *Pm69* gene regions, as well as multiple structural rearrangements (Figure 6 and Supplemental Figure 16; Supplemental Table 15). Within 0.5–3.1-Mb physical intervals comprising these clusters, G305-3M ONT contigs harbored 47 NLRs and the Zavitan reference genome contained 42 NLRs, whereas all other domesticated wheat genome assemblies contained eight to 24 NLRs (Supplemental Table 15). Moreover, orthologous NLR clusters were also identified in chromosome groups 6A (6–23 NLRs) and 6D (7–19 NLRs). Interestingly, the stem rust resistance protein Sr13, cloned from chromosome 6A of *T. durum* (Zhang et al., 2017; Gill et al., 2021), belongs to this homoeologous NLR cluster. Although PM69 is close to Sr13 in an evolutionary tree of all cloned functional R-proteins from *Triticeae* (Supplemental Figure 17), their protein sequence similarity is low (49%), suggesting that they are not true orthologs. Evolutionary analysis of 744 NLRs from these PM69 homologous/orthologous clusters in 23 wheat genomes classified them into 14 different clades (Supplemental Figure 18). PM69 belongs to clade 12, which contains 47 proteins that might be identified as its homologs/orthologs, whereas Sr13 is present in clade 11 with 90 proteins. Together, our results show that *Pm69* resides in a rapidly evolving NLR cluster that exhibits abundant genetic variation and complex rearrangement events, which increased the complexity of gene cloning.

A search for *Pm69* homologs in the ONT genome assembly of G305-3M identified a homolog that is highly similar to *Pm69* (NLR9, 92% similarity) on contig utg5064 within the *Pm69* NLR cluster (Supplemental Figure 19A), suggesting a duplication event. Blasting the cDNA sequence of *Pm69* against the WEW_v.2.0 reference genome revealed three copies on chromosome 6B in the range of 717–718 Mbp, with DNA identity >92% in exon 1 and >86% in exon 2 (Supplemental Figure 19B). Moreover, one to two duplicated copies of *pm69* were annotated in several wheat reference genomes (Figure 6). Other NLRs in the cluster also showed two to 13 duplication events with different arrangement orders in different wheat

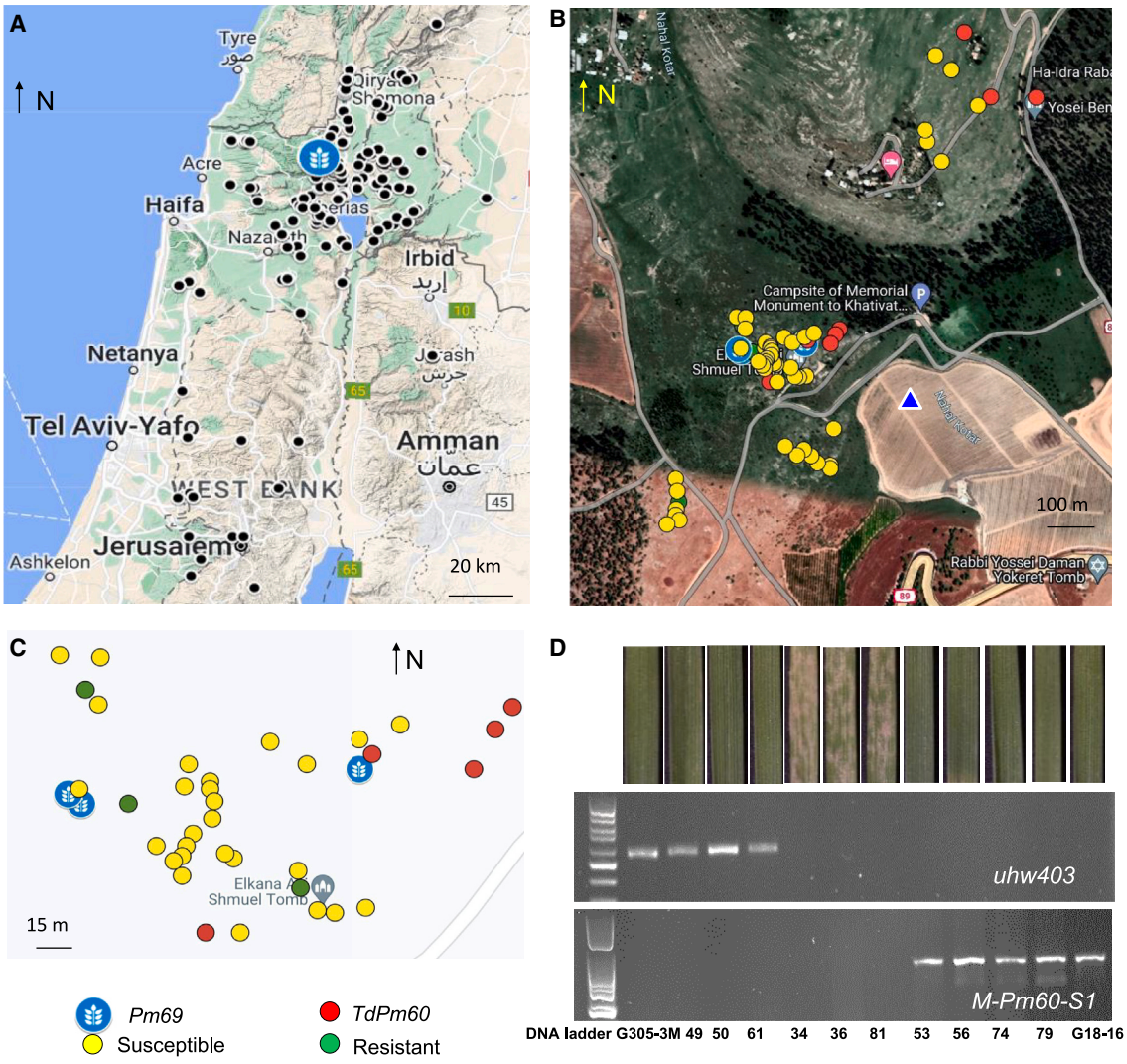

Figure 5. Geographic distribution of the *Pm69* allele in WEW populations.

(A) Geographic distribution of WEW collections (black circles) that were screened for the presence of the *Pm69* functional allele.

(B) Geographic distribution of individual WEW plants collected near the recorded G305-3M collection site (marked by a blue triangle, south of Kadita, Northern Israel).

(C) A submap of **(B)** shows that only three accessions contained *Pm69*. The maps were obtained from Google Maps.

(D) Phenotypes in response to *Bgt* #70 and agarose gel electrophoresis of PCR products amplified by markers *uhw403* (549 bp for *Pm69*) and *M-Pm60-S1* (831 bp for *TdPm60*) from representative WEW accessions.

genomes (Figure 6). These duplication and rearrangement events provide additional evidence for the rapid evolution of the *Pm69* NLR cluster.

The *Pm69* NLR cluster also contains one to two copies of 12-oxophytodienoate reductase 11 (OPR11), which is known to be involved in the biosynthesis of jasmonic acid. In contrast to the rapid evolution of the NLRs, OPR11 exhibits a highly conserved protein sequence among different wheat genomes (Supplemental Table 16), suggesting an opposing evolutionary force. Moreover, more distant regions flanking the *Pm69* clusters showed high collinearity, with similar gene content and order in different wheat genomes, implying that strong evolutionary forces may act on NLRs, probably imposed by natural selection (Figure 6).

Introgression of *Pm69* into cultivated wheat and pyramiding with a yellow rust R-gene

As part of the aim to develop resistant pre-breeding genetic resources, we transferred *Pm69* into the elite Israeli bread wheat cultivar 'Ruta' using marker-assisted selection following the "durum as a bridge" approach (Klymiuk et al., 2019) (Supplemental Figure 20; Supplemental Table 17). We also introgressed *Pm69* into the durum wheat cultivar 'Svevo,' which contains *Sr13b* (Gill et al., 2021). These homozygous introgression lines with different segments of the G305-3M chromosome were selected from BC_4F_2 populations and showed high resistance to *Bgt* #70 (Figure 7A; Supplemental Table 17).

Moreover, we found that G305-3M contains the yellow rust R-gene *Yr15*, which was confirmed by our ONT sequencing data,

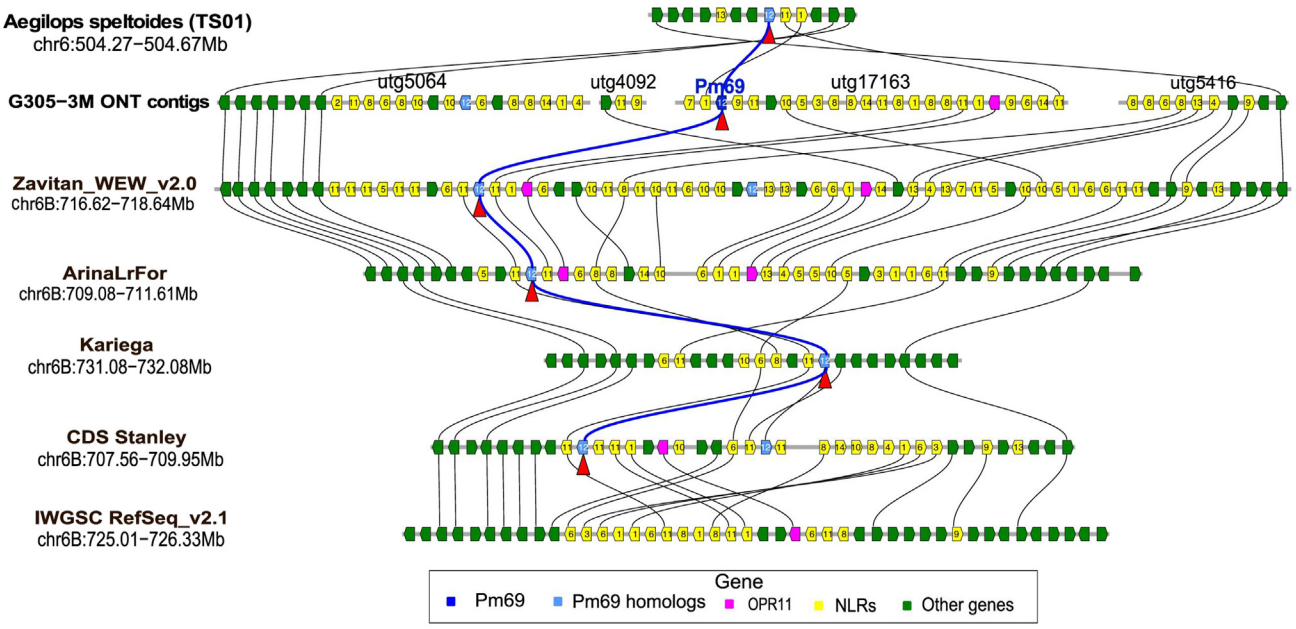

Figure 6. Microcollinearity analysis of the *Pm69* NLR cluster region among different *Triticeae* genomes.
Black lines connect genes with high collinearity, and blue lines connect *Pm69* and its homologs. The numbers on the yellow NLRs represent different NLR clades based on the evolutionary analysis. NLRs with the same number probably evolved from duplication events. Dark blue indicates *Pm69,* and light blue indicates *pm69* homologs. Red triangles mark the locations of *Pm69* and its most similar homologs. Pink indicates *OPR11* homologs that are more conserved than the *Pm69* homologs among different genomes. Green indicates other non-NLR proteins. The NLRs show greater genetic diversity than their flanking non-NLR proteins.

was present in the 4.57-Mbp contig utg1161, and showed high resistance to the wheat yellow rust (*Puccinia striiformis* f. sp. *tritici*) isolate *Pst* #5006 (Figure 7A). We pyramided *Pm69* with *Yr15* in the hexaploid cultivar 'Avocet' background and selected homozygous plants (Avocet*Yr15*+*Pm69*) that showed high resistance to both *Pst* #5006 (infection type [IT] = 1–3) and *Bgt* #70 (IT = 0–1) by marker-assisted selection (Figure 7A; Supplemental Table 18). The Ruta+*Pm69* line also showed high resistance to four additional *Bgt* isolates, #15, #107, #103, and #101, whereas Ruta was highly susceptible to *Bgt* #15, #103, and #101 (Supplemental Figure 21). These resistant introgression lines can be used in future wheat resistance breeding programs (Figure 7B).

DISCUSSION

The repertoire and diversity of R-genes among crop wild relatives make them a good source for resistance breeding against various diseases. The main strategies for protecting gene pools of wild relatives are (i) *in situ* conservation in nature (e.g., natural habitats), which allows them to continuously evolve novel resistance against rapidly evolving pathogens (Huang et al., 2016; Fu et al., 2019), and (ii) *ex situ* conservation via on-site collections and long-term storage at gene banks (e.g., the Institute of Evolution Wild Cereal Gene Bank [Krugman et al., 2018]). These collections can be used to identify valuable genes for wheat breeding. To date, several genes have already been cloned from *ex situ* WEW collections, including the *Pm* R-genes *Pm41* and *TdPm60*, which encode NLR immune receptors (Li et al., 2020, 2021; Wu et al., 2022); the yellow rust R-gene *Yr15* (*WTK1*), which encodes a tandem kinase-pseudokinase protein domain; and *Yr36* (*WKS1*), which encodes a protein with kinase and START lipid-binding-like domains (Fu et al., 2009; Klymiuk et al., 2018). In the current study, we cloned the *Pm69* gene from the G305-3M WEW accession that confers wide-spectrum resistance to a worldwide collection of 55 *Bgt* isolates (Supplemental Table 1). The discovery of this new R-gene provides a highly valuable resource for wheat resistance breeding.

We encountered several obstacles to cloning of *Pm69* owing to the high complexity of the polyploid wheat genome, such as structural rearrangements and rapidly evolving NLR clusters (Figures 2 and 6). Eventually, we were able to dissect the complexity of this rearranged locus by using ONT long-read sequencing technology to assemble long contigs that covered approximately 97% of the whole genome of the *Pm69* donor line G305-3M. The MutRNA-seq approach helped us to identify a *Pm69* candidate within a large NLR cluster by sequencing the transcriptome of the resistant wild-type G305-3M and its susceptible derivative mutants (Figure 3). The MutRNA-seq approach is a useful method for identifying one to two candidate genes based on comparisons of a wild-type line with four to five of its derivative independent mutants (Yu et al. 2022, 2023; Wang et al., 2023). The main advantage of this combination of long-read sequencing and RNA-seq methods is that it enables anchorage of short DNA reads to long ONT contigs, thus enabling us to determine whether two fragments belong to the same gene or separate genes. Furthermore, this method (ONT-MutRNA-seq) is suitable for cloning any type of gene for which mutants with a clear phenotype can be generated (Supplemental Figure 22).

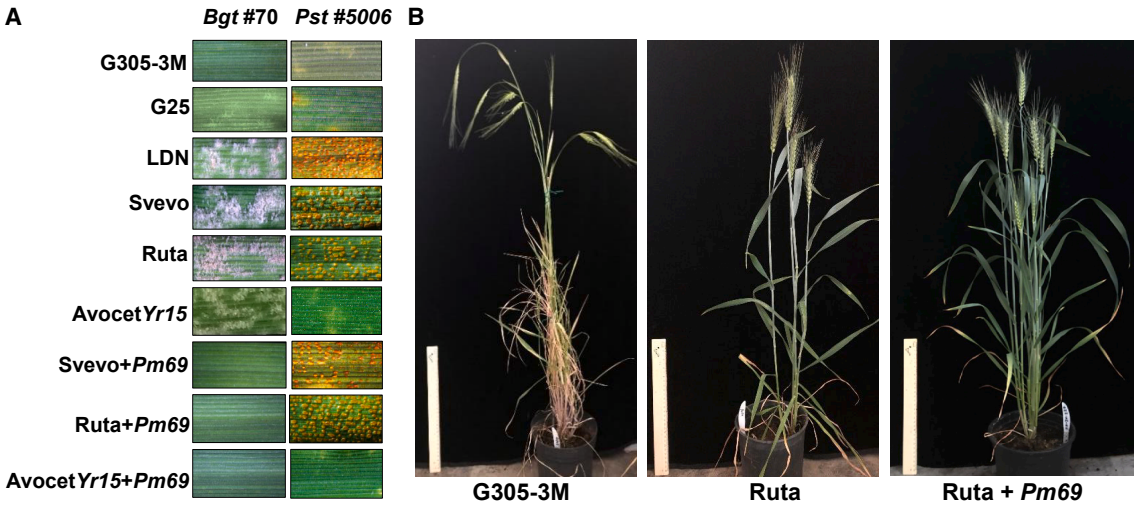

Figure 7. Introgression of *Pm69* into cultivated wheat and pyramiding with a yellow rust resistance gene.
(A) Phenotypes of different wheat parental and introgression lines to *Bgt* #70 and *Pst* #5006. WEW: G305-3M contains *Pm69* and *Yr15*, G25 contains *Yr15*. Durum wheat: LDN and Svevo. Common wheat: Ruta and Avocet*Yr15*.
(B) Whole-plant growth habits of G305-3M, Ruta, and the representative introgression line Ruta+*Pm69*. The length of the ruler is 32 cm.

The assembly of repetitive DNA and duplicated gene clusters, such as NLRs, is very challenging when relying on short-read sequencing technologies (Tørresen et al., 2019). The *Pm69* gene region in IWGSC RefSeq v.1.0 showed a large inversion compared with other reference genomes. However, this inversion was shown to be the result of an assembly error and was corrected in the second version of the IWGSC assembly (IWGSC RefSeq v.2.1) obtained by PacBio long-read sequencing (International Wheat Genome Sequencing Consortium et al., 2018; Zhu et al., 2021) (Supplemental Table 15). Similarly, the chromosome-scale assembly of the bread wheat cv. Kariega obtained by PacBio sequencing (34-fold genome) contributed to the cloning of *Yr27* (Athiyannan et al., 2022). ONT sequencing was previously used to construct the *Crr3* locus in *Brassica napus* cv. Tosca, enabling identification of a duplicated NLR candidate for a clubroot disease R-gene (Kopec et al., 2021). In the current study, ONT long-read sequencing helped to resolve the much more complex *Pm69* gene region. Therefore, with the drop in sequencing costs, long-read sequencing technologies are becoming the preferred method for gene mapping and cloning in the pan-genomic era and improving the assemblies of complex reference genomes such as wheat (Aury et al., 2022).

Gene duplications that create gene clusters are common characteristics of rapidly evolving genes, such as NLRs, which often appear to be the products of tandem duplication events, sometimes following unequal crossing over, as well as intracluster chromosomal rearrangements and gene conversion events (Barragan and Weigel, 2021). For example, the exceptionally large size of the *Phytophthora* R-gene *Rps11* (27.7 kb) in soybean resulted from several rounds of inter- and intraspecific unequal recombination in a genomic region that harbors a cluster of large NLR genes (seven to 12 NLRs) (Wang et al., 2021). In wheat, the *Pm* R-gene *MlWE74* located on chromosome arm 2BS derived from WEW was also identified within an NBS-LRR gene cluster with three to five NLRs in different wheat genomes (Zhu et al., 2022). Here, we found more than 40 NLRs in the *Pm69* gene region (1.93–2.7 Mbp) of chromosome 6B in WEW accessions (G305-3M and Zavitan), which contain about twice as many NLRs as domesticated wheat relatives (Supplemental Table 15). The diversification of NLR gene numbers in different wheat species reflects the rapid evolutionary dynamics of plant R-genes across a relatively short evolutionary timescale (Bergelson et al., 2001).

The NLR gene cluster is found not only in the *Pm69* locus on wheat chromosome arm 6BL but also in a collinear region on chromosome arm 6AL, which contains the stem rust R-gene *Sr13* (Zhang et al., 2017) within an orthologous cluster of 12 NLRs (Supplemental Table 15). These findings suggest that these NLR clusters originated from the same diploid ancestor and continued to evolve after their split into A and B genome ancestors, resulting in at least two functional genes that confer resistance to different pathogens. Furthermore, orthologous resistance alleles from different *Triticeae* species can take different routes toward functionally active genes showing different race-specific resistance, as demonstrated by the two rye genes *Pm17* and *Pm8*, located on chromosome arm 1RS, that are orthologs or close paralogs of wheat *Pm3* located on wheat chromosome arm 1AS (Yahiaoui et al., 2004; Hurni et al., 2013; Singh et al., 2018). These different NLR alleles or genes have contributed resistance to different *Bgt* isolates during the rapid co-evolution of *R–Avr* gene pairs (Frantzeskakis et al., 2020). Other genes located inside or flanking the *Pm69* NLR cluster showed high collinearity and conservation, suggesting that different evolutionary pressures may act on NLRs relative to their neighboring genes (Figure 6).

The WEW population at the original *Pm69* collection site is highly diverse, showing the presence of at least three different *Pm* genes and dozens of susceptible accessions in a radius of less than 1 km (Figure 5). *TdPm60* is a race-specific NLR gene that was found in eight plants, whereas *Pm69*, which exhibits

wide-spectrum resistance to PM, was present in only three plants (Supplemental Tables 1 and 14). Identification of different *Pm* genes in a restricted geographic location may indicate that high selection pressure caused by the pathogen is the driving force for rapid NLR evolution and emergence of novel alleles such as *Pm69*.

The *Yr15* and *Pm69* R-genes, which originated from the two WEW accessions G-25 and G305-3M, were both collected by Dr. Gerechter-Amitai in Upper Galilee, Israel, less than 5 km apart. In a retrospective of four decades, this *ex situ* collection and disease resistance identification enabled and led to the isolation and cloning of *Yr15* and *Pm69* (Gerechter-Amitai and van Silfhout, 1984; Klymiuk et al., 2019). The cloning of these genes not only provides solid evidence for the potential contribution of crop wild relatives to global food security but also prioritizes the *ex situ* conservation of this exotic germplasm in gene banks, as natural WEW habitats are becoming smaller and spatially fragmented owing to the intense development and growth of human infrastructure. We were very lucky to still find three WEW plants with *Pm69* in the natural field, although the recorded natural land site of G305-3M collection was destroyed by human infrastructure (Figure 5B). Human infrastructure continues to invade this land, and we may soon lose the *Pm69* resources forever without *ex situ* conservation.

Long-term conservation of WEW genetic reservoirs by the scientific community will assure further exploitation of useful new target genes and their introduction into cultivated crops via breeding. In some cases, NLR genes can backfire and lead to genetic incompatibilities, often resulting in hybrid necrosis, as reported for *Ne2* (*Lr13*) (Hewitt et al., 2021b; Yan et al., 2021). In wheat, specific combinations of *Pm* alleles (NLRs) can suppress each other, as in the case of rye-derived *Pm8,* which is suppressed by its wheat ortholog *Pm3* (Hurni et al., 2014). In the current study, we introgressed *Pm69* into the susceptible bread wheat cultivar Ruta and pyramided it with the stripe rust R-gene *Yr15*. We also transferred *Pm69* into a *T. durum* cv. Svevo background that contains a functional *Sr13* (Figure 7A). The resulting *Pm69* introgression lines combined with functional NLRs or WTK genes showed high resistance to *Bgt* and *Pst* (Figure 7A; Supplementary Table 18). Considering its wide spectrum of resistance to *Bgt* isolates, *Pm69* has a great potential for future wheat resistance breeding.

METHODS

Plant materials

WEW accession G305-3M (accession number: TD116180), the *Pm69* (*PmG3M*) gene donor line, was collected from Upper Galilee, Israel. G305-3M was crossed with the susceptible *T. durum* wheat line LDN to generate segregating mapping populations. An RIL population was used for construction of a sub-cM genetic linkage map. A core collection of WEW accessions, originating from Israel and the vicinity and obtained from the Wild Cereals Gene Bank (ICGB) at the University of Haifa, Israel, was screened for the presence of *Pm69* functional alleles. The modern Israeli bread wheat cultivar Ruta and the durum wheat cultivar Svevo, highly susceptible to *Bgt* #70, were used as recurrent parents for the development of hexaploid and tetraploid introgression lines. The hexaploid wheat line Avocet+Yr15 that harbors *Yr15* (Yaniv et al., 2015; Klymiuk et al., 2018) was used as the *Yr* gene donor line or as a recurrent parent for pyramiding *Pm69* with *Yr* genes.

Bgt and *Pst* inoculation and disease assessment

Bgt #70 was used in the current study for phenotyping of the *Pm69* mapping populations and EMS mutants; it showed virulence on many *Pm* genes (e.g., *Pm1a-b*, *Pm2*, *Pm3a-d*, *Pm5a-b*, *Pm6*, *Pm7*, *Pm17*, *Pm22*, *Pm30*, and *Pm1* + *Pm2* + *Pm9*) (Ben-David et al., 2016) but was avirulent on *Pm69*. *Bgt* inoculation and IT determination were performed as described previously (Li et al., 2021). The reactions to *Bgt* inoculation were examined visually, with IT recorded on a 0–4 scale at 7 days post-inoculation (dpi). Plants with an IT 0–2 (no disease colonies or spots of less than 1 mm) were considered resistant, and those with an IT 3–4 (scattered disease spots of greater than 1 mm) were susceptible. The Israeli *Pst* isolate #5006 was used for the yellow rust resistance test as described previously (Klymiuk et al., 2018). It was scored at 14 dpi using a 0–9 scale: 0–3 = resistant, none to trace sporulation; 4–6 = intermediate, light to moderate sporulation; and 7–9 = susceptible, abundant sporulation. ROS accumulation and cell death were evaluated in inoculated wheat leaves (3 dpi) as described previously (Li et al., 2023).

Development of molecular markers and construction of genetic and physical maps

Plant genomic DNA was extracted from leaves of 2- to 3-week-old wheat seedlings using the CTAB method. Primary genetic maps of *Pm69* using cleaved amplified polymorphic sequence (CAPS) and sequence-tagged site (STS) markers were developed based on the local synteny of wheat with major cereals like rice, *Brachypodium*, *Sorghum*, and barley (Raats et al., 2014). For high-resolution mapping, we used kompetitive allele-specific PCR (KASP) markers developed using PolyMarker (http://polymarker.tgac.ac.uk/) from specific SNPs identified by the wheat 90K iSelect SNP array (Illumina, San Diego, CA, USA) and the wheat 15K SNP array (Trait Genetics, Gatersleben, Germany). The IWGSC common wheat (cv. Chinese Spring) RefSeq assembly v.1.0 (International Wheat Genome Sequencing Consortium et al., 2018), Wild Emmer Genome Assembly (accession Zavitan) WEW_v.1.0 and WEW_v.2.0 (Avni et al., 2017; Zhu et al., 2019), and Durum Wheat (cv. Svevo) RefSeq Rel. 1.0 (Maccaferri et al., 2019) were used to design simple sequence repeats (SSR) markers with BatchPrimer3 website tools, as well as for development of KASP markers after verifying polymorphisms between the parental lines by Sanger sequencing of PCR products. PCR reactions were performed with 2×Taq PCR Master Mix (TIANGEN, Sichuan, China). KASP marker analysis was performed on the StepOnePlus Real-Time PCR system (Applied Biosystems, Waltham, MA, USA) as described previously (Li et al., 2021).

Pm69-flanking markers (*uhwk386* and *uhwk399*) were used to select 147 RILs ($F_{4–6}$ generations) that carried critical recombination events in the *Pm69* gene region after screening of 5500 F_2 plants (G305-3M × LDN). These RILs were used for further dissection of the target locus by the graphical genotyping approach (Distelfeld et al., 2006). Genetic distances between the detected markers and *Pm69* were calculated from genotype and phenotype data using JoinMap 5.0. The physical location of primers for each marker was identified by performing a BLAST+ search against sequences of chromosome arm 6BL from wheat reference genomes. Genetic and physical maps of *Pm69* were constructed using MapChart v.2.2.

Pm69 mutant development

To produce loss-of-function mutants of the *Pm69* gene, we mutagenized the wild emmer accession G305-3M and a homozygous resistant F_6 RIL (169B) using 0.3%–0.5% EMS treatments as described previously (Uauy et al., 2009). We generated 1530 G305-3M and 162 169B M_0 plants, which were developed to M_2 families. We inoculated 10–20 plants of each M_2 family with *Bgt* #70 to screen for susceptible mutants under screenhouse or controlled greenhouse conditions. Susceptible mutants and their resistant sister lines were selected and grown to the M_3–M_4 generation. Resistant sister lines were kept as controls for verification of the *Pm69* candidate gene. Susceptible M_3–M_4 independent mutants, one from RIL

169B and four from G305-3M EMS-treated populations, were selected and confirmed with 30 *Pm69*-flanking markers that showed the same haplotype as G305-3M, ruling out the possibility of cross-pollination from other susceptible lines.

Chromosome sorting

Mitotic metaphase chromosome suspensions were prepared from tetraploid wheat lines G305-3M and LDN and hexaploid introgression wheat line Ruta+*Pm69* (SC28RRR-26) as described previously (Vrana et al., 2000; Kubaláková et al., 2005). In brief, the cell cycle of meristematic root tip cells was synchronized using hydroxyurea, and mitotic cells were accumulated in metaphase using amiprophos-methyl. Suspensions of intact chromosomes were prepared by mechanical homogenization of 100 formaldehyde-fixed root tips in 600 μl LB01 buffer (Dpooležel et al., 1989). GAA microsatellites and/or GAA and ACG microsatellites were labeled on chromosomes by fluorescence *in situ* hybridization in suspension (FISHIS) using fluorescein isothiocyanate (FITC)-labeled oligonucleotides (Sigma, St. Louis, MO, USA) as described previously (Giorgi et al., 2013), and chromosomal DNA was stained with DAPI (4′,6-diamidino-2-phenylindole) at 2 μg/ml. Bivariate flow karyotype FITC vs. DAPI fluorescence were acquired using a FACSAria II SORP flow cytometer and sorter (Becton Dickinson Immunocytometry Systems, Franklin Lakes, NJ, USA). The samples were analyzed at rates of 1500–2000 particles s^{-1}, and different positions of sorting windows were tested on bivariate flow karyotype FITC vs. DAPI to achieve the highest purity in the sorted 6B chromosome fractions. The content of flow-sorted fractions was estimated using microscopy analysis of slides containing 1500–2000 chromosomes sorted into a 10-μl drop of primed in situ DNA labelling (PRINS) buffer (Kubaláková et al., 1997). Sorted chromosomes were identified by fluorescence *in situ hybridization* with probes for DNA repeats pSc119.2, Afa family, and 45S rDNA as described previously (Molnár et al., 2016). At least 100 chromosomes were classified for each sample using a standard karyotype (Kubaláková et al., 2005).

Oxford Nanopore and Illumina sequencing

DNA extraction and QC

High-molecular-weight (HMW) DNA was extracted from isolated nuclei and purified following a modified salting-out DNA extraction protocol (10× Genomics) (Zhang et al., 2012). Stock HMW DNA was size selected on a Blue Pippin instrument (Sage Science) with the high-pass protocol and electrophoretic conditions to retain fragments >30 kb. Eluate was bead cleaned and concentrated. Size-selected DNA samples were quantified by fluorometry (Qubit 2.0), and DNA integrity was evaluated using a TapeStation 2200 instrument (Agilent). HMW DNA samples were stored at 4°C until library preparation.

Library preparation

Long-molecule libraries (1D: ONT) were prepared following the standard 1D ligation protocol (LSK109) with minor modifications to retain and enrich HMW molecules. In brief, 1.2-μg size-selected, end-repaired HMW DNA samples were used as input for each library preparation reaction. Libraries were sequenced with an R9 flow cell on a PromethION instrument with high accuracy base-calling enabled. Illumina DNA prep libraries were prepared, indexed, and sequenced to ∼25× coverage on the NovaSeq 6000 S4 flow cell for polishing (paired-end reads: 150 bp). Raw read data were filtered for size and quality score, and approximately ∼23× coverage was used for assembly.

Genome assembly, polishing, and scaffolding

Raw fast5 files generated by ONT sequencing of G305-3M were base called using Guppy v.3.6 (ONT) to produce fastq files. Fastq files from multiple flow cells were concatenated to form a consolidated fastq file, which was then used for genome assembly using SMARTdenovo with default parameters (Liu et al., 2021). The raw assembly from SMARTdenovo was then subjected to a single round of long-read polishing using Medaka v.144 (https://github.com/nanoporetech/medaka), followed by two rounds of short-read polishing using Pilon (Walker et al., 2014). The short-read polishing helped to correct errors in the Nanopore sequencing. Assembly statistics were calculated using QUAST v.5.0.2 (https://academic.oup.com/bioinformatics/article/29/8/1072/228832).

Construction of *Pm69* physical map and comparison with other reference genomes

The co-dominant markers in the *Pm69* gene region and candidate genes from WEW_v.2.0 were used to search the contigs of the G305-3M ONT assembly, and target contigs were selected for construction of the *Pm69* physical map. New mapping markers were developed based on the polymorphism between the ONT contigs and wheat reference genomes. These markers were used to genotype the 31 representative RILs to characterize the *Pm69* physical map. The G305 ONT contigs were sliced into 1-Mb segments with pyfasta and mapped to the wild emmer assembly WEW_v.2.0 using BWA-MEM software (Li, 2013). The G305-3M ONT contigs anchored to the *Pm69* region were compared to the Zavitan (WEW_v.2.0) and Svevo RefSeq Rel. 1.0 genomes using Minimap (https://github.com/lh3/minimap2) and visualized using ggplot geom_segment on the R platform.

Transcriptome sequencing

Wheat leaf samples from the four susceptible mutants and the G305-3M resistant wild type were collected for RNA extraction 24 h after treatment with 0.1 mM 2,1,3-benzothiadiazole + 0.05% Tween-20 to increase the expression of genes associated with the plant immune system. qPCR indicated that this treatment did not change the expression of the NLR *Pm69* in the wild-type G305-3M. Samples were sequenced on the Illumina NovaSeq 6000 instrument at Novogene-UK and yielded about 40 million 150-bp paired-end reads per sample. These RNA-seq reads were aligned to the G305-3M ONT genomic DNA contigs using GSNAP with default settings, followed by sorting (Wu et al., 2016), duplicate removal, and indexing using SAMtools. Mutations were detected by visualizing the obtained bam files with the IGV genome browser, focusing on contigs that were anchored to the *Pm69* region (Robinson and Zemo jtel, 2017). We looked for regions on the contigs that had a read depth >4 along at least 1 kb and contained mutations in all susceptible mutant samples relative to the resistant G305-3M wild-type RNA reads and the reference G305-3M genome. Mutations had to be in all reads covering the site and had to have a read quality >30. A *de novo* assembly of the wild-type RNA-seq reads was obtained using Trans-ABySS software (Robertson et al., 2010).

Gene annotations, cloning of *Pm69,* and Sanger sequencing

Gene annotation of the ONT contigs mapped to the *Pm69*-flanking region was performed on the GeneSAS 6.0 server (https://www.gensas.org/gensas) using BLAST for expressed sequence tags (EST) matching and Augustus for structural prediction. R-genes were annotated using NLR annotator (Steuernagel et al., 2020), PfamScan (ftp://ftp.ebi.ac.uk/pub/databases/Pfam/Tools/), Fgenesh gene finder (http://www.softberry.com/berry.phtml), and NCBI BLASTP. Primers for cloning and sequencing of *Pm69* were designed using ONT contig utg17163 sequences and the RNA-seq assembly with BatchPrimer3 website tools. *Pm69* was amplified from a cDNA library of G305-3M using VeriFi Polymerase (PCRBIO, London, UK), then inserted into a cloning plasmid using the 5 min TA/Blunt-Zero Cloning Kit (Vazyme, Jiangsu, China) and transformed into *E. coli* strain DH5α. The plasmid was extracted with the Hybrid-Q Plasmid Rapidprep Kit (GeneAll, Seoul, Korea) and sequenced using the BigDye Terminator v1.1 Cycle Sequencing Kit (Applied Biosystems) on an ABI 3130 instrument (Applied Biosystems).

RNA extraction and quantitative real-time PCR (qRT–PCR)

Total RNA was extracted from *Bgt* #70-inoculated and non-inoculated G305-3M leaf segments collected at 10 different time points (0, 3, 6, 9, 12, 16, 24, 36, 48, and 72 hpi) using the RNeasy Plant Mini Kit (Qiagen, Hilden, Germany). cDNA was synthesized from total RNA using a qScript cDNA

Synthesis Kit (Quantabio, Beverly, MA, USA). Gene-specific primers for *Pm69* and the housekeeping gene *Ubiquitin* were used for quantitative real-time PCR amplification performed on a StepOne thermal cycler (ABI, Los Angeles, CA, USA) in a volume of 10 μl that contained 5 μl SYBR Green FastMix (Quantabio), 250 nM primers, and an optimized dilution of cDNA template. The program included an initial step at 95°C for 30 s, followed by 40 cycles of 95°C for 15 s, 60°C for 30 s, and 72°C for 10 s. Relative expression of the target genes was calculated as $2^{(\text{ubiquitin CT}-\text{Target CT})} \pm$ standard error of the mean. All qRT–PCRs were performed in triplicate, each with five independent biological repetitions.

VIGS

VIGS vector construction and inoculation were performed as described previously (Yuan et al., 2011). To specifically silence the *Pm69* gene without off-target effects on the G305-3M transcriptome, we used si-Fi software to predict 150–350 nt gene regions with efficient small interfering RNAs (Lück et al., 2019). Two selected regions were amplified and inserted into the *pCa-BSMV-γ* vector, and insertions of *GFP* and *PDS* were performed to generate controls. Equimolar amounts of *Agrobacterium tumefaciens* strain GV3101 with *pCa-BSMV-α*, *pCa-BSMV-β*, and *pCa-BSMV-γ* vectors carrying target or control genes were used to inoculate *Nicotiana benthamiana* leaves to produce virus transcripts. Sap was then extracted from infiltrated *N. benthamiana* leaves and used to inoculate the second leaves of 2-week-old wheat plantlets. When the pCa-BSMV-γ-PDS-silenced plants showed leaf chlorosis, the plants were inoculated with *Bgt* #70 in a growth chamber. Two weeks post-inoculation, the reaction of wheat plants to *Bgt* inoculation was recorded.

Phylogeny and synteny analysis

An evolutionary tree was built with MEGA X (alignment with MUSCLE, neighbor-joining algorithm), and the tree was drawn using iTOL v.6 (https://itol.embl.de/). The neighbor-joining tree was built from protein sequences of genes in the NLR cluster using MAFFT and FastTree. Synteny was analyzed with TGT (http://wheat.cau.edu.cn/TGT/). PM69 homologs/orthologs were identified by blasting the PM69 protein sequence against the WheatOmics 1.0, EnsemblPlants, and NCBI databases. PM69 homologs were aligned with the multiple alignment tool CLUSTALW from NCBI and displayed using ESPript (https://espript.ibcp.fr/ESPript/cgi-bin/ESPript.cgi).

Statistical analysis

Statistical analysis was performed using JMP v.15.1 statistical packages (SAS Institute, Cary, NC, USA). Comparisons between treatments were performed using Student's *t*-test. Asterisks indicate the level of significance: *$p < 0.05$, **$p < 0.01$, and ***$p < 0.001$.

DATA AVAILABILITY

The ONT contigs of wild emmer wheat G305-3M have been submitted to the Zenodo database under https://doi.org/10.5281/zenodo.7254921. Raw reads from MutRNA-seq have been deposited at the NCBI Sequence Read Archive under BioProject ID PRJNA795708. The *Pm69* gene sequence has been deposited at NCBI GeneBank with ID OP846108 and is attached at the end of the supplemental information file. Correspondence and requests for materials and data should be addressed to Tzion Fahima.

SUPPLEMENTAL INFORMATION

Supplemental information is available at *Plant Communications Online*.

FUNDING

T.F. was supported by the Israel Science Foundation, grant numbers 2289/16, 1366/18, and 2342/18, and the United States–Israel Binational Science Foundation (2019654). C.J.P. was supported by the Genome Canada–funded project 4D Wheat. I.M. and J.D. were supported by the ERDF project Plants as a Tool for Sustainable Global Development (no. CZ.02.1.01/0.0/0.0/16_019/0000827). G.C. and T.F. were supported by the United States National Science Foundation (1937855) and the United States Department of Agriculture (2020-67013-32577). Y.L. was supported by a fellowship provided by the Planning and Budgeting Committee (PBC) of the Israel Council for Higher Education for Outstanding Postdoctoral Fellows from China and India.

AUTHOR CONTRIBUTIONS

T.F. conceived the study; T.F., C.J.P., H.S., and Y.L. designed the experimental approach; Z.-Z.W., Y.L., R.B.-D., V.B., and V.K. developed the critical RILs and genetic maps; Z.-Z.W., Y.L., V.B., and S.J. developed and screened the mutants; J.D. and I.M. performed chromosome flow sorting; C.J.P., H.S.C., J.E., and K.W. performed ONT sequencing and assembly; Y.L., H.S., and R.R. performed the MutRNA-seq; Y.L. and R.R. performed qPCR and *Pm69* cloning; Y.L., H.S., and L.G. performed the VIGS; Y.L. and Z.-Z.W. developed the introgression lines; Y.L., Y.Z., and H.S. conducted the evolutionary analysis; Y.L., Z.-Z.W., S.J., L.G., and V.K. performed the phenotyping for *Bgt* and *Pst* resistance; L.Y., P.B.P., Z.-Z.W., and H.S. analyzed *Pm69* alleles in the different wheat accessions; Y.L., T.F., H.S., and Z.-Z.W. drafted the manuscript; T.F., C.J.P., G.C., J.D., L.G., V.K., H.S.C., J.E., K.W., R.B.-D., and R.R. reviewed and edited the manuscript; T.F. was responsible for the coordination and funding acquisition.

ACKNOWLEDGMENTS

The authors wish to thank Dr. Olga Borzov, Dr. Tamar Kis-papo, Dr. Tamar Krugman, and Ms. Souad Khalifa for their professional and moral support; Dr. Mahmoud Said, Zdeňka Dubská, and Jitka Weiserová for their assistance with chromosome sorting; Dr. Imad Shams and Dr. Tamar Lotan Labs for assistance in microscopy work; Dr. Amir Raz and Prof. Avi Levy for providing the VIGS plasmids and Nicotiana benthamiana seeds; Andrew G. Sharpe and Chu Shin Koh for their assistance with raw ONT assembly; Dr. Lin Huang for assistance in screening for the distribution of Pm69 in wheat accessions; and Dr. Weilong Guo and Yongming Chen for their assistance with the evolutionary analysis. The University of Haifa has filed a patent application (number PCT/IL2023/050137) on the use of the sequences of the powdery mildew resistance gene that is based on the results described here and on which T.F., Y.L., Z.-Z.W., and L.G. are listed as inventors.

Received: March 22, 2023
Revised: May 10, 2023
Accepted: July 4, 2023
Published: July 6, 2023

REFERENCES

Amarasinghe, S.L., Su, S., Dong, X., Zappia, L., Ritchie, M.E., and Gouil, Q. (2020). Opportunities and challenges in long-read sequencing data analysis. Genome Biol. **21**:30.

Andersen, E.J., Nepal, M.P., Purintun, J.M., Nelson, D., Mermigka, G., and Sarris, P.F. (2020). Wheat disease resistance genes and their diversification through integrated domain fusions. Front. Genet. **11**:898.

Arora, S., Steuernagel, B., Gaurav, K., Chandramohan, S., Long, Y., Matny, O., Johnson, R., Enk, J., Periyannan, S., Singh, N., et al. (2019). Resistance gene cloning from a wild crop relative by sequence capture and association genetics. Nat. Biotechnol. **37**:139–143.

Athiyannan, N., Abrouk, M., Boshoff, W.H.P., Cauet, S., Rodde, N., Kudrna, D., Mohammed, N., Bettgenhaeuser, J., Botha, K.S., Derman, S.S., et al. (2022). Long-read genome sequencing of bread wheat facilitates disease resistance gene cloning. Nat. Genet. **54**:227–231.

Aury, J.M., Engelen, S., Istace, B., Monat, C., Lasserre-Zuber, P., Belser, C., Cruaud, C., Rimbert, H., Leroy, P., Arribat, S., et al. (2022). Long-read and chromosome-scale assembly of the hexaploid

wheat genome achieves high resolution for research and breeding. GigaScience **11**:giac034.

Avni, R., Nave, M., Barad, O., Baruch, K., Twardziok, S.O., Gundlach, H., Hale, I., Mascher, M., Spannagl, M., Wiebe, K., et al. (2017). Wild emmer genome architecture and diversity elucidate wheat evolution and domestication. Science **357**:93–97.

Barragan, A.C., and Weigel, D. (2021). Plant NLR diversity: the known unknowns of pan-NLRomes. Plant Cell **33**:814–831.

Ben-David, R., Parks, R., Dinoor, A., Kosman, E., Wicker, T., Keller, B., and Cowger, C. (2016). Differentiation among *Blumeria graminis* f. sp. *tritici* isolates originating from wild versus domesticated Triticum species in Israel. Phytopathology **106**:861–870.

Bergelson, J., Kreitman, M., Stahl, E.A., and Tian, D. (2001). Evolutionary dynamics of plant R-genes. Science **292**:2281–2285.

Bohra, A., Kilian, B., Sivasankar, S., Caccamo, M., Mba, C., McCouch, S.R., and Varshney, R.K. (2021). Reap the crop wild relatives for breeding future crops. Trends Biotechnol. **40**:412–431.

Deamer, D., Akeson, M., and Branton, D. (2016). Three decades of nanopore sequencing. Nat. Biotechnol. **34**:518–524.

Distelfeld, A., Uauy, C., Fahima, T., and Dubcovsky, J. (2006). Physical map of the wheat high-grain protein content gene *Gpc-B1* and development of a high-throughput molecular marker. New Phytol. **169**:753–763.

Dpooležel, J., Binarová, P., and Lcretti, S. (1989). Analysis of Nuclear DNA content in plant cells by Flow cytometry. Biol. Plant. (Prague) **31**:113–120.

Frantzeskakis, L., Di Pietro, A., Rep, M., Schirawski, J., Wu, C.H., and Panstruga, R. (2020). Rapid evolution in plant–microbe interactions – a molecular genomics perspective. New Phytol. **225**:1134–1142.

Fu, D., Uauy, C., Distelfeld, A., Blechl, A., Epstein, L., Chen, X., Sela, H., Fahima, T., and Dubcovsky, J. (2009). A kinase-START gene confers temperature-dependent resistance to wheat stripe rust. Science **323**:1357–1360.

Fu, Y.B., Peterson, G.W., Horbach, C., Konkin, D.J., Beiles, A., and Nevo, E. (2019). Elevated mutation and selection in wild emmer wheat in response to 28 years of global warming. Proc. Natl. Acad. Sci. USA **116**:20002–20008.

Gaurav, K., Arora, S., Silva, P., Sánchez-Martín, J., Horsnell, R., Gao, L., Brar, G.S., Widrig, V., John Raupp, W., Singh, N., et al. (2022). Population genomic analysis of *Aegilops tauschii* identifies targets for bread wheat improvement. Nat. Biotechnol. **40**:422–431.

Gerechter-Amitai, Z.K., and van Silfhout, C.H. (1984). Resistance to powdery mildew in wild emmer (*Triticum dicoccoides* Körn.). Euphytica **33**:273–280.

Gill, B.K., Klindworth, D.L., Rouse, M.N., Zhang, J., Zhang, Q., Sharma, J.S., Chu, C., Long, Y., Chao, S., Olivera, P.D., et al. (2021). Function and evolution of allelic variations of *Sr13* conferring resistance to stem rust in tetraploid wheat (*Triticum turgidum* L.). Plant J. **106**:1674–1691.

Giorgi, D., Farina, A., Grosso, V., Gennaro, A., Ceoloni, C., and Lucretti, S. (2013). FISHIS: Fluorescence In Situ Hybridization in Suspension and Chromosome Flow Sorting Made Easy. PLoS One **8**, e57994.

Golzar, H., Shankar, M., and D'Antuono, M. (2016). Responses of commercial wheat varieties and differential lines to western Australian powdery mildew (*Blumeria graminis* f. Sp. *tritici*) populations. Australas. Plant Pathol. **45**:347–355.

Hewitt, T., Müller, M.C., Molnár, I., Mascher, M., Holušová, K., Šimková, H., Kunz, L., Zhang, J., Li, J., Bhatt, D., et al. (2021a). A highly differentiated region of wheat chromosome 7AL encodes a *Pm1a* immune receptor that recognizes its corresponding *AvrPm1a* effector from Blumeria. New Phytol. **229**:2812–2826.

Hewitt, T., Zhang, J., Huang, L., Upadhyaya, N., Li, J., Park, R., Hoxha, S., McIntosh, R., Lagudah, E., and Zhang, P. (2021b). Wheat leaf rust resistance gene *Lr13* is a specific *Ne2* allele for hybrid necrosis. Mol. Plant **14**:1025–1028.

Holzberg, S., Brosio, P., Gross, C., and Pogue, G.P. (2002). Barley stripe mosaic virus-induced gene silencing in a monocot plant. Plant J. **30**:315–327.

Huang, L., Raats, D., Sela, H., Klymiuk, V., Lidzbarsky, G., Feng, L., Krugman, T., and Fahima, T. (2016). Evolution and Adaptation of Wild Emmer Wheat Populations to Biotic and Abiotic Stresses. Annu. Rev. Phytopathol. **54**:279–301.

Hurni, S., Brunner, S., Buchmann, G., Herren, G., Jordan, T., Krukowski, P., Wicker, T., Yahiaoui, N., Mago, R., and Keller, B. (2013). Rye *Pm8* and wheat *Pm3* are orthologous genes and show evolutionary conservation of resistance function against powdery mildew. Plant J. **76**:957–969.

Hurni, S., Brunner, S., Stirnweis, D., Herren, G., Peditto, D., McIntosh, R.A., and Keller, B. (2014). The powdery mildew resistance gene *Pm8* derived from rye is suppressed by its wheat ortholog *Pm3*. Plant J. **79**:904–913.

International Wheat Genome Sequencing Consortium (IWGSC), Appels, R., Eversole, K., Stein, N., Feuillet, C., Keller, B., Rogers, J., Pozniak, C.J., Choulet, F., Distelfeld, A., et al. (2018). Shifting the limits in wheat research and breeding using a fully annotated reference genome. Science **361**, eaar7191.

Jumper, J., Evans, R., Pritzel, A., Green, T., Figurnov, M., Ronneberger, O., Tunyasuvunakool, K., Bates, R., Žídek, A., Potapenko, A., et al. (2021). Highly accurate protein structure prediction with AlphaFold. Nature **596**:583–589.

Klymiuk, V., Fatiukha, A., Huang, L., Wei, Z., Kis-Papo, T., Saranga, Y., Krugman, T., and Fahima, T. (2019). Durum Wheat as a Bridge between Wild Emmer Wheat Genetic Resources and Bread Wheat. In Applications of Genetic and Genomic Research in Cereals (Woodhead Publishing), pp. 201–230.

Klymiuk, V., Yaniv, E., Huang, L., Raats, D., Fatiukha, A., Chen, S., Feng, L., Frenkel, Z., Krugman, T., Lidzbarsky, G., et al. (2018). Cloning of the wheat *Yr15* resistance gene sheds light on the plant tandem kinase-pseudokinase family. Nat. Commun. **9**:3735.

Kopec, P.M., Mikolajczyk, K., Jajor, E., Perek, A., Nowakowska, J., Obermeier, C., Chawla, H.S., Korbas, M., Bartkowiak-Broda, I., and Karlowski, W.M. (2021). Local Duplication of TIR-NBS-LRR Gene Marks Clubroot Resistance in *Brassica napus* cv. Tosca. *Front. Plant Sci.* **12**:639631.

Krattinger, S.G., Lagudah, E.S., Spielmeyer, W., Singh, R.P., Huerta-Espino, J., McFadden, H., Bossolini, E., Selter, L.L., and Keller, B. (2009). A putative ABC transporter confers durable resistance to multiple fungal pathogens in wheat. Science **323**:1360–1363.

Krugman, T., Nevo, E., Beharav, A., Sela, H., and Fahima, T. (2018). The Institute of Evolution Wild Cereal Gene Bank at the University of Haifa. Isr. J. Plant Sci. **65**:129–146.

Kubaláková, M., Macas, J., and Doležel, J. (1997). Mapping of repeated DNA sequences in plant chromosomes by PRINS and C-PRINS. Theor. Appl. Genet. **94**:758–763.

Kubaláková, M., Kovárová, P., Suchánková, P., Číhalíková, J., Bartoš, J., Lucretti, S., Watanabe, N., Kianian, S.F., and Doležel, J. (2005). Chromosome Sorting in Tetraploid Wheat and Its Potential for Genome Analysis. Genetics **170**:823–829.

Li, H. (2013). Aligning sequence reads, clone sequences and assembly contigs with BWA-MEM. Preprint at arXiv. https://doi.org/10.48550/arxiv.1303.3997.

Li, M., Dong, L., Li, B., Wang, Z., Xie, J., Qiu, D., Li, Y., Shi, W., Yang, L., Wu, Q., et al. (2020). A CNL protein in wild emmer wheat confers powdery mildew resistance. New Phytol. **228**:1027–1037.

Li, Y., Roychowdhury, R., Govta, L., et al. (2023). Intracellular reactive oxygen species-aided localized cell death contributing to immune responses against wheat powdery Mildew pathogen. Phytopathology **113**:884–892.

Li, Y., Wei, Z.Z., Fatiukha, A., Jaiwar, S., Wang, H., Hasan, S., Liu, Z., Sela, H., Krugman, T., and Fahima, T. (2021). *TdPm60* identified in wild emmer wheat is an ortholog of *Pm60* and constitutes a strong candidate for *PmG16* powdery mildew resistance. Theor. Appl. Genet. **134**:2777–2793.

Li, L.F., Zhang, Z.B., Wang, Z.H., Li, N., Sha, Y., Wang, X.F., Ding, N., Li, Y., Zhao, J., Wu, Y., et al. (2022). Genome sequences of five Sitopsis species of Aegilops and the origin of polyploid wheat B subgenome. Mol. Plant **15**:488–503.

Liu, H., Wu, S., Li, A., and Ruan, J. (2021). SMARTdenovo: A de novo Assembler Using Long Noisy Reads. Gigabyte **2021**:1–9.

Lu, P., Guo, L., Wang, Z., Li, B., Li, J., Li, Y., Qiu, D., Shi, W., Yang, L., Wang, N., et al. (2020). A rare gain of function mutation in a wheat tandem kinase confers resistance to powdery mildew. Nat. Commun. **11**:680.

Lück, S., Kreszies, T., Strickert, M., Schweizer, P., Kuhlmann, M., and Douchkov, D. (2019). siRNA-Finder (si-Fi) Software for RNAi-Target Design and Off-Target Prediction. Front. Plant Sci. **10**:1023.

Maccaferri, M., Harris, N.S., Twardziok, S.O., Pasam, R.K., Gundlach, H., Spannagl, M., Ormanbekova, D., Lux, T., Prade, V.M., Milner, S.G., et al. (2019). Durum wheat genome highlights past domestication signatures and future improvement targets. Nat. Genet. **51**:885–895.

Mascher, M., Wicker, T., Jenkins, J., Plott, C., Lux, T., Koh, C.S., Ens, J., Gundlach, H., Boston, L.B., Tulpová, Z., et al. (2021). Long-read sequence assembly: a technical evaluation in barley. Plant Cell **33**:1888–1906.

McIntosh, R.A., Dubcovsky, J., Rogers, W.J., Xia, X.C., and Raupp, W.J. (2020). Catalogue of gene symbols for wheat: 2020 supplement. Annu. Wheat Newsl. **66**:116–117.

Molnár, I., Kubaláková, M., Šimková, H., Farkas, A., Cseh, A., Megyeri, M., Vrána, J., Molnár-Láng, M., and Doležel, J. (2014). Flow cytometric chromosome sorting from diploid progenitors of bread wheat, *T. urartu, Ae. speltoides* and. Theor. Appl. Genet. **127**:1091–1104.

Molnár, I., Vrána, J., Burešová, V., Cápal, P., Farkas, A., Darkó, É., Cseh, A., Kubaláková, M., Molnár-Láng, M., and Doležel, J. (2016). Dissecting the U, M, S and C genomes of wild relatives of bread wheat (*Aegilops* spp.) into chromosomes and exploring their synteny with wheat. Plant J. **88**:452–467.

Moore, J.W., Herrera-Foessel, S., Lan, C., Schnippenkoetter, W., Ayliffe, M., Huerta-Espino, J., Lillemo, M., Viccars, L., Milne, R., Periyannan, S., et al. (2015). A recently evolved hexose transporter variant confers resistance to multiple pathogens in wheat. Nat. Genet. **47**:1494–1498.

Nilsen, K.T., Walkowiak, S., Xiang, D., Gao, P., Quilichini, T.D., Willick, I.R., Byrns, B., N'Diaye, A., Ens, J., Wiebe, K., et al. (2020). Copy number variation of *TdDof* controls solid-stemmed architecture in wheat. Proc. Natl. Acad. Sci. USA **117**:28708–28718.

Raats, D., Yaniv, E., Distelfeld, A., Ben-David, R., Shanir, J., Bocharova, V., Schulman, A., and Fahima, T. (2014). Application of CAPS Markers for Genomic Studies in Wild Emmer Wheat. In Cleaved Amplified Polymorphic Sequences (CAPS) Markers in Plant Biology (New York: Nova Science Publishers), pp. 31–60.

Rairdan, G.J., Collier, S.M., Sacco, M.A., Baldwin, T.T., Boettrich, T., and Moffett, P. (2008). The coiled-coil and nucleotide binding domains of the potato Rx disease resistance protein function in pathogen recognition and signaling. Plant Cell **20**:739–751.

Rhoads, A., and Au, K.F. (2015). PacBio sequencing and its applications. Dev. Reprod. Biol. **13**:278–289.

Robertson, G., Schein, J., Chiu, R., Corbett, R., Field, M., Jackman, S.D., Mungall, K., Lee, S., Okada, H.M., Qian, J.Q., et al. (2010). De novo assembly and analysis of RNA-seq data. Nat. Methods **7**:909–912.

Robinson, P., and Zemo jtel, T. (2017). Integrative genomics viewer (IGV): Visualizing alignments and variants. In Computational Exome and Genome Analysis (Chapman and Hall/CRC), pp. 233–245.

Sánchez-Martín, J., Steuernagel, B., Ghosh, S., Herren, G., Hurni, S., Adamski, N., Vrána, J., Kubaláková, M., Krattinger, S.G., Wicker, T., et al. (2016). Rapid gene isolation in barley and wheat by mutant chromosome sequencing. Genome Biol. **17**:221.

Sánchez-Martín, J., Widrig, V., Herren, G., Wicker, T., Zbinden, H., Gronnier, J., Spörri, L., Praz, C.R., Heuberger, M., Kolodziej, M.C., et al. (2021). Wheat *Pm4* resistance to powdery mildew is controlled by alternative splice variants encoding chimeric proteins. Nat. Plants **7**:327–341.

Sato, K., Abe, F., Mascher, M., Haberer, G., Gundlach, H., Spannagl, M., Shirasawa, K., and Isobe, S. (2021). Chromosome-scale genome assembly of the transformation-amenable common wheat cultivar "Fielder. DNA Res. **28**:dsab008.

Shizuya, H., Birren, B., Kim, U.-J., Mancino, V., Slepak, T., Tachiiri, Y., and Simon, M. (1992). Cloning and stable maintenance of 300-kilobase-pair fragments of human DNA in Escherichia coli using an F-factor-based vector. Proc. Natl. Acad. Sci. USA **89**:8794–8797.

Singh, S.P., Hurni, S., Ruinelli, M., Brunner, S., Sanchez-Martin, J., Krukowski, P., Peditto, D., Buchmann, G., Zbinden, H., and Keller, B. (2018). Evolutionary divergence of the rye *Pm17* and *Pm8* resistance genes reveals ancient diversity. Plant Mol. Biol. **98**:249–260.

Steuernagel, B., Witek, K., Krattinger, S.G., Ramirez-Gonzalez, R.H., Schoonbeek, H.J., Yu, G., Baggs, E., Witek, A.I., Yadav, I., Krasileva, K.v., et al. (2020). The NLR-Annotator Tool Enables Annotation of the Intracellular Immune Receptor Repertoire. Plant Physiol. **183**:468–482.

Steuernagel, B., Periyannan, S.K., Hernández-Pinzón, I., Witek, K., Rouse, M.N., Yu, G., Hatta, A., Ayliffe, M., Bariana, H., Jones, J.D.G., et al. (2016). Rapid cloning of disease-resistance genes in plants using mutagenesis and sequence capture. Nat. Biotechnol. **34**:652–655.

Thind, A.K., Wicker, T., Šimková, H., Fossati, D., Moullet, O., Brabant, C., Vrána, J., Doležel, J., and Krattinger, S.G. (2017). Rapid cloning of genes in hexaploid wheat using cultivar-specific long-range chromosome assembly. Nat. Biotechnol. **35**:793–796.

Tørresen, O.K., Star, B., Mier, P., Andrade-Navarro, M.A., Bateman, A., Jarnot, P., Gruca, A., Grynberg, M., Kajava, A.v., Promponas, V.J., et al. (2019). Tandem repeats lead to sequence assembly errors and impose multi-level challenges for genome and protein databases. Nucleic Acids Res. **47**:10994–11006.

Uauy, C., Paraiso, F., Colasuonno, P., Tran, R.K., Tsai, H., Berardi, S., Comai, L., and Dubcovsky, J. (2009). A modified TILLING approach to detect induced mutations in tetraploid and hexaploid wheat. BMC Plant Biol. **9**:115.

Vrána, J., Kubaláková, M., Simková, H., Cíhalíková, J., Lysák, M.A., and Dolezel, J. (2000). Flow sorting of mitotic chromosomes in common wheat (*Triticum aestivum* L.). Genetics **156**:2033–2041.

Walker, B.J., Abeel, T., Shea, T., et al. (2014). Pilon: an integrated tool for comprehensive microbial variant detection and genome assembly improvement. PLoS One **9**, e112963.

Walkowiak, S., Gao, L., Monat, C., Haberer, G., Kassa, M.T., Brinton, J., Ramirez-Gonzalez, R.H., Kolodziej, M.C., Delorean, E., Thambugala, D., et al. (2020). Multiple wheat genomes reveal global variation in modern breeding. Nature **588**:277–283.

Wang, W., Chen, L., Fengler, K., Bolar, J., Llaca, V., Wang, X., Clark, C.B., Fleury, T.J., Myrvold, J., Oneal, D., et al. (2021). A giant NLR gene confers broad-spectrum resistance to *Phytophthora sojae* in soybean. Nat. Commun. **12**:6263.

Wang, Y., Abrouk, M., Gourdoupis, S., Karaaátová, M., Karafiátová, M., Molnár, I., Holušová, K., Doležel, J., Athiyannan, N., Cavalet-Giorsa, E., et al. (2023). An unusual tandem kinase fusion protein confers leaf rust resistance in wheat. Nat. Genet. **55**:914–920.

Wei, Z.Z., Klymiuk, V., Bocharova, V., Pozniak, C., and Fahima, T. (2020). A post-haustorial defense mechanism is mediated by the powdery mildew resistance gene, *PmG3M*, derived from wild emmer wheat. Pathogens **9**:418.

Wu, T.D., Reeder, J., Lawrence, M., Becker, G., and Brauer, M.J. (2016). GMAP and GSNAP for genomic sequence alignment: Enhancements to speed, accuracy, and functionality. In Methods in Molecular Biology, pp. 283–334.

Wu, Q., Zhao, F., Chen, Y., Zhang, P., Zhang, H., Guo, G., Xie, J., Dong, L., Lu, P., Li, M., et al. (2021). Bulked segregant CGT-Seq-facilitated map-based cloning of a powdery mildew resistance gene originating from wild emmer wheat (*Triticum dicoccoides*). Plant Biotechnol. J. **19**:1288–1290.

Wu, Q., Chen, Y., Li, B., Li, J., Zhang, P., Xie, J., Zhang, H., Guo, G., Lu, P., Li, M., et al. (2022). Functional characterization of powdery mildew resistance gene *MlIW172*, a new *Pm60* allele and its allelic variation in wild emmer wheat. J. Genet. Genomics **49**:787–795.

Xie, W., Ben-David, R., Zeng, B., Distelfeld, A., Röder, M.S., Dinoor, A., and Fahima, T. (2012). Identification and characterization of a novel powdery mildew resistance gene *PmG3M* derived from wild emmer wheat. Theor. Appl. Genet. **124**:911–922.

Xie, J., Guo, G., Wang, Y., Hu, T., Wang, L., Li, J., Qiu, D., Li, Y., Wu, Q., Lu, P., et al. (2020). A rare single nucleotide variant in *Pm5e* confers powdery mildew resistance in common wheat. New Phytol. **228**:1011–1026.

Xing, L., Hu, P., Liu, J., Witek, K., Zhou, S., Xu, J., Zhou, W., Gao, L., Huang, Z., Zhang, R., et al. (2018). *Pm21* from *Haynaldia villosa* encodes a CC-NBS-LRR protein conferring powdery mildew resistance in wheat. Mol. Plant **11**:874–878.

Yahiaoui, N., Srichumpa, P., Dudler, R., and Keller, B. (2004). Genome analysis at different ploidy levels allows cloning of the powdery mildew resistance gene *Pm3b* from hexaploid wheat. Plant J. **37**:528–538.

Yan, X., Li, M., Zhang, P., Yin, G., Zhang, H., Gebrewahid, T.W., Zhang, J., Dong, L., Liu, D., Liu, Z., and Li, Z. (2021). High-temperature wheat leaf rust resistance gene *Lr13* exhibits pleiotropic effects on hybrid necrosis. Mol. Plant **14**:1029–1032.

Yaniv, E., Raats, D., Ronin, Y., Korol, A.B., Grama, A., Bariana, H., Dubcovsky, J., Schulman, A.H., and Fahima, T. (2015). Evaluation of marker-assisted selection for the stripe rust resistance gene *Yr15*, introgressed from wild emmer wheat. Mol. Breed. **35**:1–12.

Yu, G., Matny, O., Champouret, N., Steuernagel, B., Moscou, M.J., Hernández-Pinzón, I., Green, P., Hayta, S., Smedley, M., Harwood, W., et al. (2022). *Aegilops sharonensis* genome-assisted identification of stem rust resistance gene *Sr62*. Nat. Commun. **13**:1607.

Yu, G., Matny, O., Gourdoupis, S., Rayapuram, N., Aljedaani, F.R., Wang, Y.L., Nürnberger, T., Johnson, R., Crean, E.E., Saur, I.M.-L., et al. (2023). The wheat stem rust resistance gene Sr43 encodes an unusual protein kinase. Nat. Genet. **55**:921–926.

Yuan, C., Li, C., Yan, L., Jackson, A.O., Liu, Z., Han, C., Yu, J., and Li, D. (2011). A high throughput barley stripe mosaic virus vector for virus induced gene silencing in monocots and dicots. PLoS One **6**:e26468.

Zhang, M., Zhang, Y., Scheuring, C.F., Wu, C.C., Dong, J.J., and Zhang, H.B. (2012). Preparation of megabase-sized DNA from a variety of organisms using the nuclei method for advanced genomics research. Nat. Protoc. **7**:467–478.

Zhang, W., Chen, S., Abate, Z., Nirmala, J., Rouse, M.N., and Dubcovsky, J. (2017). Identification and characterization of *Sr13*, a tetraploid wheat gene that confers resistance to the Ug99 stem rust race group. Proc. Natl. Acad. Sci. USA **114**:E9483–E9492.

Zhang, J., Zhang, P., Dodds, P., and Lagudah, E. (2020). How Target-Sequence Enrichment and Sequencing (TEnSeq) Pipelines Have Catalyzed Resistance Gene Cloning in the Wheat-Rust Pathosystem. Front. Plant Sci. **11**:678.

Zhao, F., Li, Y., Yang, B., Yuan, H., Jin, C., Zhou, L., Pei, H., Zhao, L., Li, Y., Zhou, Y., et al. (2020). Powdery mildew disease resistance and marker-assisted screening at the *Pm60* locus in wild diploid wheat *Triticum urartu*. Crop J. **8**:252–259.

Zhou, Y., Bai, S., Li, H., Sun, G., Zhang, D., Ma, F., Zhao, X., Nie, F., Li, J., Chen, L., et al. (2021). Introgressing the *Aegilops tauschii* genome into wheat as a basis for cereal improvement. Nat. Plants **7**:774–786.

Zhu, T., Wang, L., Rodriguez, J.C., Deal, K.R., Avni, R., Distelfeld, A., McGuire, P.E., Dvorak, J., and Luo, M.C. (2019). Improved Genome Sequence of Wild Emmer Wheat Zavitan with the Aid of Optical Maps. G3 **9**:619–624.

Zhu, T., Wang, L., Rimbert, H., Rodriguez, J.C., Deal, K.R., de Oliveira, R., Choulet, F., Keeble-Gagnère, G., Tibbits, J., Rogers, J., et al. (2021). Optical maps refine the bread wheat *Triticum aestivum* cv. Chinese Spring genome assembly. Plant J. **107**:303–314.

Zhu, K., Li, M., Wu, H., Zhang, D., Dong, L., Wu, Q., Chen, Y., Xie, J., Lu, P., Guo, G., et al. (2022). Fine mapping of powdery mildew resistance gene *MlWE74* derived from wild emmer wheat (*Triticum turgidum* ssp. *dicoccoides*) in an NBS-LRR gene cluster. Theor. Appl. Genet. **135**:1235–1245.

Zhu, S., Liu, C., Gong, S., Chen, Z., Chen, R., Liu, T., Liu, R., Du, H., Guo, R., Li, G., et al. (2023). Orthologous genes *Pm12* and *Pm21* from two wild relatives of wheat show evolutionary conservation but divergent powdery mildew resistance. Plant Commun. **4**:100472.

Zou, S., Wang, H., Li, Y., Kong, Z., and Tang, D. (2018). The NB-LRR gene *Pm60* confers powdery mildew resistance in wheat. New Phytol. **218**:298–309.